University of Stavanger

Faculty of Science and Technology

MASTER'S THESIS

Study program/Specialization: Mathematics and Physics	Spring semester, 2016 Restricted access
Writer: Ekom Isaac Eduok	…… (Writer's signature)
Faculty supervisor: Prof. Helge Bøvik Larsen External supervisor(s):	
Thesis title: Thermal properties of geopolymer materials	
Credits (ECTS): 60	
Key words: Geopolymer Aplite ground granulated blast furnace slag Geopolymerization Retarder Microsilica Calorimetry Heat evolution	Pages: VIII + 74 + enclosure: …… Stavanger, 15 June 2016 Date/year

Thermal properties of geopolymer materials

Ekom Eduok

June 2016

MASTER'S THESIS

Institutt for matematikk og naturvitskap

Universitet i Stavanger, Norway.

Supervisor: Helge Bøvik Larsen

Abstract

Ordinary Portland cement (OPC) is traditionally the most common binder in concrete manufacturing and is widely used in the petroleum industry, yet its mechanical properties have some shortcomings and its production has proven environmentally harmful. In addition, various industries generate by-products which also have a negative environmental impact. Interested parties therefore seek to replace OPC with a superior cementitious material that can be produced through recycling industrial by-products. One potential replacement is geopolymer binders; however, the quality of the geopolymer depends on the source materials used and the specific methods for creating it.

Ground granulated blast furnace slag (GGBFS) is a by-product of iron or steel manufacturing. This research conducts a thermal analysis on the creation of an aplite-slag (GGBFS) based geopolymer, considering the effects of 1) the addition of microsilica to increase the silica/alumina ratio, and 2) the addition of sucrose as a retarder to shift the geopolymer setting time. The results indicate that increasing the soluble silicate content has a negative effect, but an optimal curing temperature tends to improve the extent of geopolymerization. Additionally, an optimum retarder dosage of sucrose was found to be 1.2% of the total solid content, which lengthened the geopolymerization process by 20.39 minutes and also increased the heat evolution by 13.3%. These adjustments would lead to better physical and mechanical properties in the final product, thus presenting an encouraging prospect in the industrial application of this material.

Preface

This is the report of the research work carried out as a requirement for M.Sc. in Physics at the University of Stavanger, Norway. This dissertation is original, unpublished, and independent work by the author. Due acknowledgement has been made to all materials used in the text.

The experimental procedures in chapter 3 was done primarily by the author, except for the mix-designs which was designed and prepared by M. Khalifeh. The data collection and analysis in chapter 4 are my original work.

_____

Ekom Eduok

Stavanger, Norway

6 June, 2016.

"You never change things by fighting the existing reality. To change something, build a new model that makes the existing model obsolete."

- Buckminster Fuller -

Acknowledgement

I would first like to thank God for being my strength and guide in the writing of this thesis. Without Him, I would not have had the wisdom or the physical ability to do so.

I express my gratitude to my thesis supervisor Prof. Helge Bøvik Larsen of the Mathematics and Natural Science at University of Stavanger. He devoted time in reading my work and consistently allowed this paper to be my own work, but steered me in the right direction with much needed motivation whenever he thought I needed it.

I would also like to thank the geopolymer experts at Institute of Petroleum Technology, University of Stavanger, who were involved in the sample design and preparation for this research project: Prof. Helge Hodne and Dr. Mahmoud Khalifeh. Without their passionate participation and input, the analysis could not have been successfully conducted.

I would also like to acknowledge Catey Hinkle of the editorial staff at the Apostolic faith world Headquarters in Portland, Oregon, as the second reader and editor of this thesis, and I am gratefully indebted to her for her very valuable comments on this thesis.

My gratitude goes to the Norwegian government who has funded my Master's Program through the Norwegian tax payers and the oil revenue.

Finally, I must express my profound gratitude to my parents and to my siblings for their unfailing support and continuous encouragement throughout my years of study and through the process of researching and writing this thesis. This accomplishment would not have been possible without them. Thank you.

Ekom Eduok

6 June, 2016.

Contents

List of terms and abbreviations

Al	Aluminum
Al^{3+}	Aluminum ion
Al_2O_3	Aluminum oxide (alumina)
API	American Petroleum Institute
ASTM	America society for testing and materials
BaO	Barium oxide
C	Carbon
Ca	Calcium
Ca^{+}	Calcium ion
CaO	Calcium oxide
CO_2	Carbon dioxide
Cr_2O_3	Chromium
C-S-H	Calcium silicate hydrate
DLTMA	Dynamic Load Thermomechanical Analysis
DMA	Dynamic Mechanical Analysis
DSC	Differential scanning calorimetry
FA	Fly ash
Fe	Iron
Fe_2O_3	Iron (III) Oxide
GGBFS	Ground granulated blast furnace slag
HM	Hydration modulus
H_2O	Water
ICTAC	International confederation for thermal analysis and calorimetry
K^{+}	Potassium ion

K_b	Basicity coefficient
K_2CO_3	Potassium carbonate
K_2O	Potassium oxide
KOH	Potassium hydroxide
K_2SO_4	Potassium sulfate
LOI	Loss on ignition
MgO	Magnesium oxide
mJ/s	Millijoule per second
MnO	Manganese (II) Oxide
MPa	Mega pascal
mW	Milliwatt
Na^+	Sodium ion
Na_2CO_3	Sodium carbonate
Na_2O	Sodium oxide
NaOH	Sodium hydroxide
Na_2SO_4	Sodium sulfate
OH^-	Hydroxide ion
OPC	Ordinary Portland cement
PFA	Pulverized fuel ash
P_2O_5	Phosphorus pentoxide
POFA	Palm oil fuel ash
RHA	Rice husk ash
RM	Red mud
RPM	Revolutions per minute
S^{-2}	Sulfide ion
Si	Silicon

Si^{4+}	Silicon ion
SiO_2	Silicon dioxide (silica)
$Si(OH)_4$	Silicon hydroxide
SiO_2K_2O	Potassium silicate
SiO_2Na_2O	Sodium silicate
SrO	Strontium oxide
TiO_2	Titanium dioxide
TMA	Thermomechanical Analysis
µl	Microlitre
µm	Micrometre

1

INTRODUCTION

1.1 Background

In recent years, there has been an alarming increase of industrial by-products generated by the rice milling industry, iron and steel making industry, power generation industry, mining industry, timber manufacturing industry, etc., and this is becoming one of the most urgent environmental issues of our time [1, 2]. The disposal of these industrial by-products contributes to land loss and also lowers the aesthetic quality of landscapes [1]. Apart from industrial waste generation, the production of ordinary Portland cement (OPC; traditionally the most-used binder in concrete manufacturing, which is widely used in the petroleum industry both for sealing the annular space between casing and formation, and zonal isolation [3]), has been questioned lately due to the environmental impact of clinker [4, 5].

During the production of Portland cement clinker, there is an extensive consumption of energy in which large amounts of greenhouse gases (CO_2) are released into the atmosphere [6]. In fact, it has been reported that up to 1.5 billion tons of CO_2 are emitted annually from OPC manufacturing worldwide, which accounts for around 5% of total man-made CO_2 emissions [7, 8]. This has prompted various studies in an attempt to reduce global carbon emissions and to promote large-volume recycling of waste materials into new industrial products that could replace OPC. The benefits of recycling vary depending on the materials and the form of recycling [9].

Of late, one waste recycling option that has grown in importance in research and development is geopolymer binders [2]. Geopolymer binders are a type of green cementitious material introduced in 1972 by Joseph Davidovits to identify the reaction product between alkaline solutions (such as sodium hydroxide [NaOH], potassium hydroxide [KOH], sodium silicate [SiO_2Na_2O] or potassium silicate [SiO_2K_2O]) and a source material of geological origin or a by-product material

rich in silica and alumina (such as fly ash, rice-husk ash, aplite, ground granulated blast furnace slag [GGBFS], metakaolin, etc.) [10, 11]. It has been shown by other research works [12, 13] that after hardening, geopolymers possess excellent mechanical properties, fire resistance, and anticorrosion. For instance, GGBFS, an industrial by-product of iron or steel manufacturing, has been used significantly in the production of a geopolymer concrete with superior mechanical properties [14, 15]. Fly ash, also known as pulverized fuel ash (PFA), is a by-product of coal burning power plants that has also been found to yield a geopolymer concrete with excellent strength compared to OPC concrete [16-18]. Other industrial by-products such as red mud (RM) from the aluminum refining industry, palm oil fuel ash (POFA) from the palm oil industry, rice husk ash (RHA) from the rice milling industry, etc. [16, 19-21], have also found their way into the production of geopolymer concrete. A detailed description of these materials and its chemical compositions is given in Chapter 2 and Chapter 3.

Thus, the ever-present burden of reducing the use of OPC in construction and in the petroleum industry because of its greenhouse gas emissions, possible gas influx (permeability), autogenous shrinking, instability at high temperatures or in a corrosive environment, etc., is coupled with the problem of how to dispose of industrial by-products generated by various industries. Green cementitious materials could address both of these challenges, and therefore have a high potential for replacing OPC as the main binder in the future of concrete technology [2, 22, 23].

1.2 Objective of the research

The objective of this research is to conduct a thermal analysis on a geopolymer slurry using a differential scanning calorimetry (DSC) technique, focusing solely on an aplite-slag (GGBFS) based geopolymer, along with various effects such as 1) the addition of microsilica to increase the silica/alumina ratio, and 2) the addition of sucrose as a retarder to shift the geopolymer setting time. Focus was put on the heat evolution of the geopolymer slurry and the resulting chemical reactions at borehole control temperature (50°C), to characterize the thermal properties of the geopolymerization process from the time it is pumped as a slurry into the borehole, to the time it is completely polymerized. The dynamic and isothermal segments of the DSC machine were used

to gradually raise the temperature of the geopolymer slurry from ambient (25°C) to borehole control temperature (50°C).

The focus was then expanded to cover the heat evolution of the geopolymer slurry and the chemical reactions connected to this at ambient temperature (25°C).

Thermal analysis is a technique that can be used in characterizing the mechanical behavior of geopolymers, by analyzing the amount of heat evolved during the geopolymerization process and associating this heat evolution to the mechanical properties of the final geopolymeric structure. The heat evolution and mechanical properties of geopolymers have been observed to be positively correlated [24].

Limitations

This study is limited to an aplite-slag based geopolymer, and does not include other geopolymeric source materials. It is also limited to a geopolymer slurry and does not include already-formed geopolymeric structures. Some hypothesis are made in the course of this work, and further research and experiments are needed to ascertain their validity. This will be explicitly commented upon.
The modelling has been carried out in an "ideal" laboratory environment, thus avoiding a number of phenomena such as for instance, elevated pressure and confined space.

1.3 Outline of the thesis

The first chapter of this report is a literature review of topics related to this experimental work and its results. The second chapter is a detailed discussion of all the experimental methods used in this project. The third chapter is a presentation of the results, discussion, and finally the concluding remarks.
A list of all the terms and abbreviations used in this thesis can be found on Page VI.

For further information about geopolymers and their applications, *Geopolymer Chemistry and Applications* [11] should be consulted. Relevant information about thermal analyses and differential scanning calorimetry can be found in *Thermal Analysis in Practice* [25].

2

THE GEOPOLYMER

2.1 Brief historical development

Following a series of catastrophic fires in Europe between 1970-1973, French scientist, Joseph Davidovits, was prompted to research materials that could be developed as a fire-resistant alternative to organic thermosetting polymers [26, 27]. This led to the successful development of a new material coined ***geopolymer***.

Figure 2.1: Catastrophic fire involving plastics in 1970 [27].

To the ordinary user, geopolymers are essentially the same as polymers. Like organic polymers, they are transformed, undergo polycondensation, and set rapidly at a low temperature. But in addition, they are GEO-polymers. That means they are hard, inorganic, non-inflammable, and stable at temperatures up to 1250°C [27]. This new material gave a tremendous boost to innovation, as seen in Fig. 2.2, and has also found its application as a heat-resistant adhesive [28, 29], as a

coating for fire protection for cruise ships [26] and for various other purposes. However, its primary application has since shifted to uses in construction, as published by Wastiels et al. [30]. There is also ongoing research regarding how this product could replace OPC in the petroleum industry.

Figure 2.2: Decorative items made of (K)-Poly (sialate-siloxo) geopolymer binder [27].

2.2 Geopolymer binders

Davidovits [31, 32] proposed that silicon (Si) and aluminum (Al) present in a source material of geological origin or in by-product materials such as GGBFS and fly ash could be used to react with an alkaline liquid to produce binders. Since the chemical reaction involved in this case is a polymerization process, he named it ***geopolymer*** to represent these binders. Thus, geopolymers belong to the inorganic polymers family.

There has been intensive research on alkali-activated binders as an alternative to OPC due to its low environmental impact, acid resistance, and high mechanical properties, among other advantageous qualities. This was confirmed by Davidovits [27] when he observed that geopolymers harden rapidly at room temperature and gain a compressive strength of up to 20MPa after 4 hours. Hardjito et al. [33] conducted a similar study using coal fly ash as a geopolymer binder, reporting that geopolymer binders perform better than OPC binders and proving their suitability for replacing OPC. Most studies [34-41] have indicated that factors such as Al_2O_3/SiO_2 ratio (aluminum oxide/ silicon oxide), water/solid ratio, alkali concentration, curing temperature with curing time play an important role in the strength of geopolymers.

2.3 Constituents of geopolymer binders

The two main constituents of geopolymers are alkaline liquids and source materials. The alkaline liquids come from soluble alkali metals that are usually potassium or sodium based. A combination of sodium hydroxide (NaOH) or potassium hydroxide (KOH) and sodium silicate [SiO_2Na_2O] or potassium silicate [SiO_2K_2O] is the most common alkaline liquid used in geopolymerization. The source materials that are the primary requirements for geopolymerization to occur are materials that are rich in silicon (Si) and aluminum (Al) [41]. These can be industrial by-product materials such as fly ash, GGBFS, red mud, silica fume, rice-husk ash, etc. Alternatively, natural minerals such as aplite or metakaolin could also be used as source materials. The choice of the source materials for geopolymerization depends on the type of application, cost, availability, specific demands of the end users, and other similar factors [42].

Based on the above considerations, many researchers have studied the geopolymerization and effect of different mix-designs, various combinations of natural minerals and industrial by-product materials, the addition of a chemical admixture in geopolymer binders, and a variety of ways to improve the polymerization process (see for example [43-47]). For this thesis, an aplite-slag based geopolymer with an admixture such as sucrose is used.

2.3.1 Blast furnace slag

Slags are industrial by-products resulting from the iron manufacturing process. They consist mainly of alumino-silicate glass and calcium-magnesium, although their properties and chemical compositions vary depending on the raw materials that were used and the manufacturing process [48]. One commonly used slag is ground granulated blast furnace slag (GGBFS), which is another industrial by-product obtained by rapid water cooling of molten steel to produce a glassy material that is ground into fine powder. The main components of GGBFS include magnesium oxide (MgO), silica (SiO_2), alumina (Al_2O_3), and calcium oxide (CaO) [48].

Slags can be activated in an alkaline medium to produce geopolymeric products. A typical alkaline-activated slag product yields a highly amorphous calcium silicate hydrate (C-S-H) gel product which has a high aluminum content, is highly resistant to chemical attack, and has excellent thermal properties [49].

2.3.2 Aplite

Aplite is an intrusive[1] igneous rock with the same mineral component as granite, but with a much finer grain [50]. The main constituents of aplite includes quartz, alkali-feldspar[2], microcline, and albite.

Aplite has found its application in concrete material for strength development, and has recently been used as a source material for geopolymer cement [23]. Its low aluminum content restricts it as a stand-alone source material, but it has been used with calcium and aluminum-rich GGBFS for appropriate geopolymerization [23].

2.3.3 Alkaline activators

An alkaline activators are one of the most important factors in the production of a green cementitious material with excellent mechanical properties through the geopolymerization process. The alkaline solution is what controls the initial mechanism of the reaction by leaching alumina and silica species from the source material into the solution, and thereby prompting precipitation and crystallization of the aluminosilicate species present in the solution [2]. The metal cations (typically Na^+ and/or K^+) present in the alkaline medium form a structural element with the aluminosilicate geopolymeric gels and charge balance the tetrahedral aluminum (AlO_4^-) negative framework [51] while the hydroxide ion (OH^-) acts as a catalyst for reactivity [2].

When aluminosilicate source materials are mixed in an alkaline medium, dissolution and gelation of the aluminosilicate species happens quickly, resulting in less time for the formation of a crystalline structure. As a result, an amorphous, semi-amorphous, or micro-crystalline structures are formed [41].

Common alkaline activators include NaOH, Na_2SO_4, waterglass, Na_2CO_3, K_2CO_3, KOH, and K_2SO_4 [41], while the most-utilized alkaline activators are mixtures of potassium or sodium hydroxides (NaOH, KOH) with potassium waterglass (SiO_2K_2O) or sodium waterglass (SiO_2Na_2O) respectively [52].

The most critical factor for the formation of a geopolymer structure with excellent mechanical properties, is the concentration of the alkaline activator. It is well known [2] that an increase in the

[1] Intrusive rocks are formed within Earth's crust from the crystallization of magma.
[2] Feldspar are minerals such as anorthoclase and orthoclase, which are rich in alkali elements (potassium and sodium).

concentration of the activator will lead to an increase in the reaction rate, resulting in a less-porous and stronger geopolymer cement. Yet, there is an optimum concentration limit for a given geopolymeric material with a given activator (see for example [2, 41]). Crossing this limit leads to a reverse effect as excess hydroxide will cause the precipitation of the aluminosilicate gel at a very early stage, resulting in a lower-strength geopolymer [2].

2.3.4 Chemical Admixture

Some properties of a geopolymer may be changed by adding chemical admixtures at the mixing stage. Admixtures are commonly used to increase workability, adjust the setting or hardening time, and to adjust other properties such as mechanical strength.

The most commonly used admixtures include accelerators and retarders. An accelerator shortens the setting time of a cementitious material, thereby increasing the strength buildup [53]. The most widely used accelerators in geopolymer concrete include calcium chloride and sodium salts [47]. Retarders are added in geopolymeric mixtures to delay the setting time by retarding the reaction rate of the geopolymerization process [10], especially in high calcium content source material where rapid stiffening interferes with the polymerization process, leading to a reduction in geopolymer mechanical strength. The most widely used retarder is sucrose.

In this analysis, more emphasis will be given to retarders since they are an integral part of the mix-design used in this thesis work.

In a sucrose-based admixture, the HO-C-C=O groups from sucrose is converted into acid complexes by the alkaline medium. The source material present in this aqueous medium absorbs the acid complexes, mostly by Ca^{+} ions[3], sealing off the calcium complex nucleating sites from the alkaline solution causing retardation. In addition, Sucrose also retard the geopolymerization process by reacting with Fe, Al, and Ca in the mixture to form insoluble metal organic complexes which is adsorbed onto the surfaces of the source particles [22].

[3] The leaching of Ca^{+} ions into the aqueous medium normally causes the rapid stiffening of the geopolymer which disrupt further dissolution of alumina and silica species.

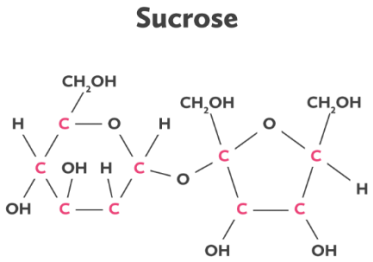

Figure 2.3: Molecular structure of sucrose [54].

2.4 The geopolymerization: a conceptual model

To understand the thermal properties of a reacting geopolymer slurry, it is necessary to have an understanding of the chemical reactions involved in geopolymerization—the complicated process that is responsible for the formation of a geopolymer. The mechanism involved has been studied for decades, yet the exact process is still not fully understood [26, 51].

In the 1950s, Glukhovsky [55] tried to explain geopolymerization by proposing a general model to describe the process controlling the formation of aluminosilicate materials in alkali medium. The model is divided into three stages:

- destruction–coagulation
- coagulation–condensation
- condensation–crystallization

This process involves a substantially fast chemical reaction under alkaline conditions with Si and Al minerals, resulting in a three-dimensional polymeric chain-and-ring structure which consists of Si-O-Al-O bonds [7].

2.4.1 First Stage: Destruction–Coagulation

The first stage is the dissolution of the solid aluminosilicate source by breaking the Si-O-Si, Al-O-Al, and Al-O-Si bonds in the source material. The breaking of the Si-O-Si and Al-O-Al bonds can only be attained in a strong alkaline medium[4]. The rupture of the Si-O-Si bond is caused by the presence of hydroxyl group ions (OH^-) in the alkaline medium [26]:

[4] Dissolution of the alumina-silica species is rapid at a high pH level, thereby creating a quick supersaturation aluminosilicate solution.

$$\equiv Si\text{-}O\text{-}Si\equiv + OH^- \rightarrow \equiv Si\text{-}O\text{-}Si\equiv \rightarrow \equiv Si\text{-}OH + {}^-O\text{-}Si\equiv$$
$$\Big|$$
$$OH^-$$

(Eq. 2-1)

The redistribution of electron density around the silicon atom, which is caused by the action of OH^-, makes the Si-O-Si bond more prone to rupture [26]. The silicon hydroxylation forms intermediate complexes which decompose into silica-hydroxyl species and oligomers such as $Si(OH)_4$ and $OSi(OH)_3^-$ [26, 56, 57]. The alkaline metal cations that is presence in the alkaline medium, balances the resulting negative charge[5]. In the same way, the hydroxyl groups affect the Al-O-Si bond and the aluminate in the solution forms complexes, mainly $Al(OH)_4^-$. This process generates rapid heat (Fig. 2.4) and is directly proportional to the pH level of the activating solution [52]. This is in line with the findings of Yao et al. [58] who studied the geopolymerization process of alkali–metakaolinite characterized by isothermal calorimetry. Their study observed an exothermic attack of the hydroxyl groups on the oxides to produce alumina/silica-hydroxy species and oligomers, such as those mentioned above.

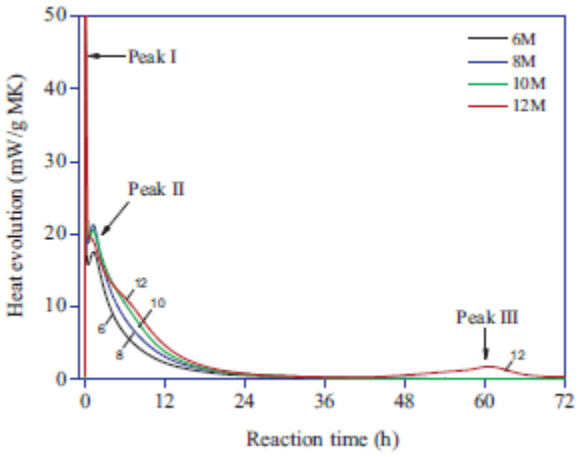

Figure 2.4: Rapid heat release during dissolution of solid particles (peak I) in the alkaline medium. The amount of heat release during dissolution is proportional to the pH of the activated solution [59].

[5] This is observed in the appearance of $\equiv Si\text{-}O^-\text{-}M^+$ bond, which hinders the formation of siloxane bonds from the reverse reaction. Where M^+ stand for either Na^+ or K^+.

2.4.2 Second Stage: Coagulation–Condensation

In this stage, the leached products from the first stage incorporate into the aqueous phase[6] and accumulate to form a coagulated structure[7] where polycondensation takes place [51]. In the case of the Si-O-Si bond which ruptured in the first stage to form the hydroxylated complex $Si(OH)_4$, during the second stage it condenses to form a new Si-O-Si bond and produces the following dimers [26]:

$$(HO)_3Si\text{-}O^- + Si\text{-}OH \rightarrow [(HO)_3Si\text{-}O \text{ ..... } Si\text{-}OH] \rightarrow [(HO)_3Si\text{-}O\text{-}\ Si\text{-}OH]^- \rightarrow$$
$$\rightarrow [(HO)_3Si\text{-}O\text{-}\ Si.....OH]^- \rightarrow (HO)_3Si\text{-}O\text{-}Si(OH)_3 + OH^-$$

(Eq. 2-2)

Aluminate also has a part in this polymerization reaction. It is worth noting that the OH^- which acted as a catalyst for destruction in the first stage acts as a structural component in the second and third stages [26] as seen in Equation 2-2.

2.4.3 Third Stage: Condensation–Crystallization

In order to explain in detail the formation of a geopolymer, many authors have recently expanded on the Gluhhovsky model and have introduced a model similar to those observed in zeolite[8] synthesis [60-63]. Their model included the two stages found in zeolite synthesis:

[6] The aqueous phase may already contain silicate if it was present in the activating solution. The addition of silicate in the activation solution provides higher silicate content, due to which the gel formation is likely to provide faster polymerization.
[7] A complex mixture of silicate, aluminate, and aluminosilicate.
[8] Zeolites are hydrated aluminosilicate minerals made from interlinked tetrahedra of alumina (AlO_4) and silica (SiO_4). That is, they are solids with a three-dimensional crystal structure synthesized from the elements aluminum, oxygen, and silicon, with alkaline metals.

— First, during a nucleation stage the aluminosilicates from the source material disintegrate in the alkaline medium, resulting in the formation of zeolite precursors[9].

— In the second stage, several nuclei grow to a critical size where crystals begin to develop.

Figure 2.5 shows the different stages involved in the transformation of aluminosilicate source materials into an alkaline-activated geopolymer. Though the stages are shown linearly, these stages can hardly be separated for they may occur simultaneously [58]. It is worth noting that the dissolution of the solid particle at the surface of the source material is the mechanism that governs the conversion of the solid particle during geopolymerization, liberating aluminosilicate species as monomers into the alkaline solution [51].

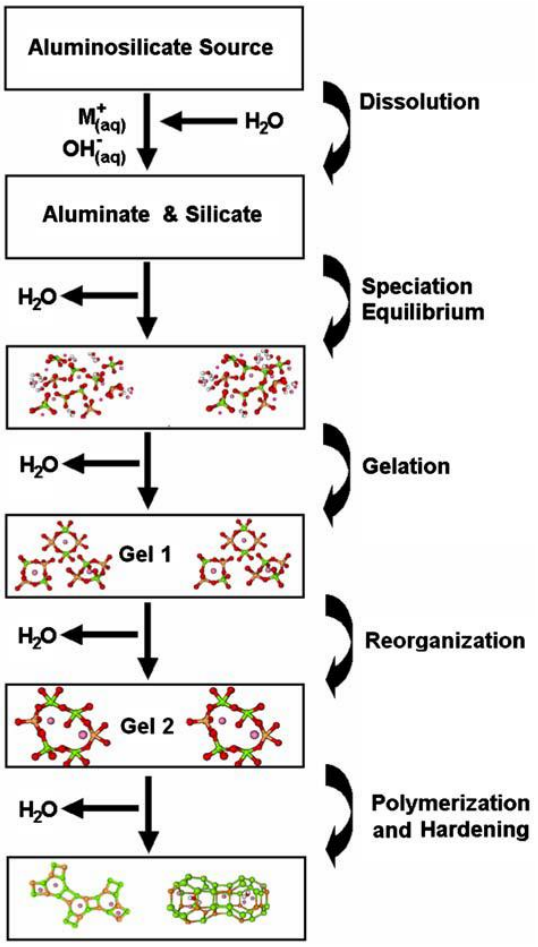

Figure 2.5: A conceptual model for geopolymerization [51].

[9] This stage is comprised of Gluhhovsky's first two stages and depends mostly on thermodynamic parameters such as temperature.

These monomers inter-react to form dimers, which also inter-react with other monomers to form trimers, tetramers, and higher molecules, yielding the polymeric covalent bonding of poly(siloxonate) Si-O-Si-O, poly(sialate) Si-O-Al-O and poly(sialate-disiloxo) Si-O-Al-O-Si-O-Si-O [26]. This results in a gelation process in the solution phase, leading to the precipitation of an aluminosilicate gel when the solution reaches saturation. This greatly hinders further dissolution of the aluminosilicate species from the solid particle surfaces to the bulk of the geopolymer, implying that unreacted aluminosilicate source particles will be present in the binder[10] [64]. This can be seen in Figure 2.6, which shows the smooth binder phase (after solidification is complete) of a geopolymer specimen, with voids where the very soft unreacted solid particles have been removed during polishing.

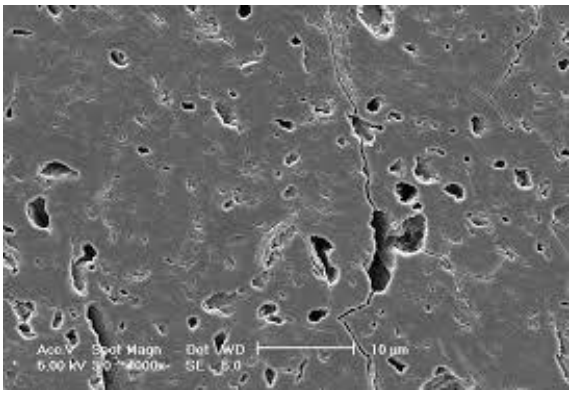

Figure 2.6: SEM micrograph of a geopolymer with unreacted solid particles [65].

The first gel to form is called Gel 1 (see Figure 2.5) and is an aluminum-rich gel. As the reaction progresses, more silicon is leached from the solid source. This results in an increased silicon concentration in the medium, which leads to the formation of Gel 2. This process has been confirmed by many researchers [26, 66, 67] as having a high concentration of Al^{3+} ions present in the alkaline medium in the early stages of the process. Fernandez et al. [61] attributed this rapid

[10] This is mostly observed in high calcium content source materials which interfere with the geopolymerization process and alter the microstructure due to rapid stiffening, resulting in the reduction of geopolymer binder mechanical strength [22]. Hence, a low calcium source material is preferred.

dissolution of aluminium over silicon to the nature of Al-O bonds being weaker than Si-O bonds, and therefor easier to break.

After gelation, the system continues to rearrange and reorganize, resulting in an increase in the connectivity of the gel network and eventually hardening. This leads to the formation of a three-dimensional aluminosilicate network commonly attributed to geopolymer materials [24, 68].

Many physical properties of this material depend on its microstructure and pore distribution, which in turn depend on the processes of structural reorganization [69].

2.5 Structural characterization

Geopolymerization is exothermic[11] and the formation of the three-dimensional macromolecular structure is assumed to be synthesized through oligomers (dimers and trimers) which provide the actual unit structure. This can be schematized as shown in Equation 2-3 and Equation 2-4 [70, 71].

$$n(Si_2O_5Al_2O_2) + 2nSiO_2 + 4nH_2O + NaOH \text{ or } KOH \rightarrow n(OH)_3\text{-Si-O-Al}^{(-)}\text{-O-Si-(OH)}_3$$

(Si-Al materials)

$$\vert$$

$$(OH)_2$$

(geopolymer precursor)

(Eq. 2-3)

$$\vert \quad \vert \quad \vert$$

$$n(OH)_3\text{-Si-O-Al}^{(-)}\text{-O-Si-(OH)}_3 + NaOH \text{ or } KOH \rightarrow (Na,K)^{(+)}\text{-(-Si-O-Al}^{(-)}\text{-O-Si-O-)} + 4nH_2O$$

$$\vert \qquad \vert \quad \vert \quad \vert$$

$$(OH)_2 \qquad O \quad O \quad O$$

$$\vert \quad \vert \quad \vert$$

(geopolymer backbone)

(Eq. 2-4)

[11] Exothermic reaction is a reaction that releases energy usually in the form of heat or light from a system to its surrounding.

According to Rangan [72], the last term of Equation 2-4 shows that during the formation of geopolymers, the water that was initially consumed during dissolution is released. This water, expelled from the geopolymer matrix during curing and drying, leaves discontinuous nanopores in the matrix which are beneficial to the geopolymer's performance. Hence, the addition of water to the geopolymer mixture plays no role in the chemical-reaction process, but does contribute to the workability of the mixture during handling [42].

The general empirical formula for this three-dimensional macromolecular framework is as follows [73]:

$$M_n\,[-(SiO_2)_z - AlO_2]_n,\, wH_2O \qquad \text{(Eq. 2-5)}$$

In this equation "M" stands for cation such as sodium, calcium, or potassium; "n" is the degree of polycondensation; "z" is number of silicate units (1,2,3 or >>3); and "w" is number of water molecules. Such a framework for the chemical designation of geopolymers based on silico-aluminates was suggested as poly(sialate) by Davidovits [70].

More details on the geopolymer's structural characterization is given in Appendix A.

2.6 Thermal analysis and calorimetry

The International Confederation for Thermal Analysis and Calorimetry **(ICTAC)** defines "thermal analysis and calorimetry" as:

> ". . . a group of techniques in which a property[12] of a sample is monitored against time or temperature while the temperature of the sample is programmed. The sample is kept in a specified atmosphere.
>
> The **temperature program** may involve heating or cooling at a fixed rate of temperature change, or holding the temperature constant, or any sequence of these" [25].

Thermal analysis involves the whole thermoanalytical method, which has two key aspects: 1) the thermoanalytical technique, or the measurement of the change in a sample property; and 2) the thermoanalytical investigation procedure, which is the interpretation and evaluation of the measured values.

2.6.1 A brief history of thermal analysis

Thermoanalytical methods were being used even before people could quantify hot and cold. This is seen in the work of the ancient Greeks [74] Philo, of Byzantium, and Heron, of Alexandria, who in the first century B.C. recognized the expansion of air caused by heat and made a simple thermometer.

In 1594 Galileo Galilei invented the first air thermoscope, followed by a two-bulbed J-shaped thermometer invented by Cornelis J. Drebbel between 1598 and 1622 [74]. In 1626, Jean Leurechon described a thermoscope equipped with a scale marked with eight degrees as a "thermometer" [74].

The evolution of thermoanalysis continued into the 19th century, and eventually the difference between enthalpy and temperature was clarified by the thermodynamic principle. Thus it became possible to measure heat quantities. In 1915, Honda measured the mass of a sample in almost continuous measurement using thermogravimetric analysis, and later in 1915, Boersma invented

[12] Any physical or chemical property of the sample.

the heat flow differential scanning calorimetry (DSC), which is presently used to analyze the thermal properties of different materials [25].

Today, numerous important properties of geopolymers can be quantitatively determined using different thermoanalytical methods such as thermomechanical analysis (TMA), dynamic load thermomechanical analysis (DLTMA), dynamic mechanical analysis (DMA), and DSC. This thesis will focus solely on the use of DSC to characterize the thermal properties of geopolymers.

2.6.2 Differential Scanning Calorimetry

DSC is a thermal analysis technique that uses a device (called a differential scanning calorimeter) to measure the temperature and heat flow (energy changes) which occur in a sample when it is heated, cooled, or held isothermally at constant temperature. This technique allows: 1) the detection of endothermic and exothermic effects; 2) the measurement of peak areas (transition and reaction enthalpy); and 3) the determination of the temperature that characterizes the peak and other effects [25].

DSC is a universal method for investigating chemical reactions and physical transitions associated with the generation or consumption of heat. The reaction heat, or heat flow rates, and their changes at characteristic temperatures can be easily measured on small sample masses (milligram range) with a sufficiently high accuracy. DSC is applied in areas such as thermal characterization (in particular polymers), stability investigation, and purity determination [75].

2.6.2.1 The DSC measurement principle

The differential scanning calorimetry consists of two small sample holders: one for an empty reference[13] pan and the other for sample material. Energy in the form of heat is applied to these sample holders independently by a very small furnace made up of pure silver with an electrical flat heater (see Figure 2.7). The temperature of each of the sample holders is then monitored by a DSC sensor consisting of a thermocouple arranged radially beneath each of the sample holders [25]. More or less heat flow is supplied to the sample holder consisting of a sample material in order to compensate for heat absorbed or evolved by the sample material. This adjustment of the heat flow

[13] The reference is usually an inert material such as empty aluminum pan.

provides a varying heat flow which is opposite but equivalent to the varying thermal behavior of the sample.

2.6.2.1.1 Heat flow measurement

The flow of energy into or out of a sample as a function of time or temperature, known as heat flow, is the main property measured by DSC. The heat flow is usually shown in mW. Because mW is mJ/s, it is literally the flow of energy in unit time [76].

The DSC sensors allow heat to flow radially through its thermal resistance R_{th}. The radially arranged thermocouple measures the temperature difference across the thermal resistance in each of the sample holders.

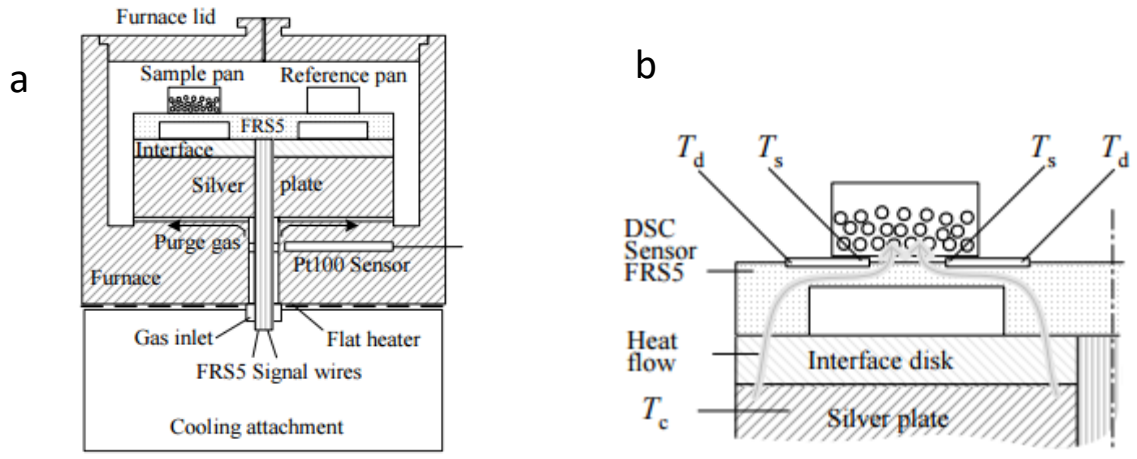

Fig 2.7: a) a cross-section of a DSC measuring cell, and b) an amplified section of the sample holder. The gray path is the heat flow direction from the silver plate of the furnace to the DSC sensor. The measured temperature difference T_s-T_d signal is equal to the heat flow on the sample holder. For the empty reference holder, T_r-T_d is the measured temperature signal, which is equal to the heat flow on the reference holder [25].

The heat flow, Q, supplied to the sample holder consisting of the sample material is given in Equation 2-6 [25] according to Ohms' law.

$$Q_1 = \frac{T_s - T_c}{R_{th}}$$

(Eq. 2-6)

Similarly, the heat supplied to the empty reference pan is given as [25]:

$$Q_2 = \frac{T_r - T_c}{R_{th}}$$

(Eq. 2-7)

Where T_c, T_s, T_r, and R_{th} are the furnace temperature, sample holder/ sample material temperature, empty reference holder temperature, and thermal resistance of the DSC sensors, respectively.

The difference between the two heat flows corresponds to the heat flow to the sample, Q, which is the DSC signal.

$$Q = Q_1 - Q_2 = \frac{T_s - T_c}{R_{th}} - \frac{T_r - T_c}{R_{th}}$$

(Eq. 2-8)

The thermal resistance of the empty reference pan and the sample holder are identical due to their symmetrical arrangement and shared T_c [25]. Hence, Equation 2-8 can be deduce to

$$Q = \frac{T_s - T_r}{R_{th}}$$

(Eq. 2-9)

However, the sensitivity of the thermocouple (which measures the temperature differences of the two sample holders) is given as, $\mathbf{S = V/\Delta T}$ [25]. It then follows that

$$Q = \frac{V}{R_{th}S} = \frac{V}{E}$$

(Eq. 2-10)

Where E is the calorimetric sensitivity of the sensor (product of R_{th} and S) and V is the thermoelectric voltage (the sensor signal).

The heat flow over time results in DSC curves (a graphical display of the heat flow), and its integral corresponds to the enthalpy change, $\Delta\mathbf{H}$, of the sample at constant pressure, as given in Equation 2-11 and Equation 2-12 [25].

$$\left(\frac{dQ}{dt}\right)p = \frac{dH}{dt} \qquad \text{(Eq. 2-11)}$$

Where $\left(\frac{dQ}{dt}\right)_p$ is the amount of heat evolved or absorbed (heat flow) at constant pressure and is equal to the enthalpy change $\frac{dH}{dt}$. A schematic diagram of DSC is shown in Figure 2.8.

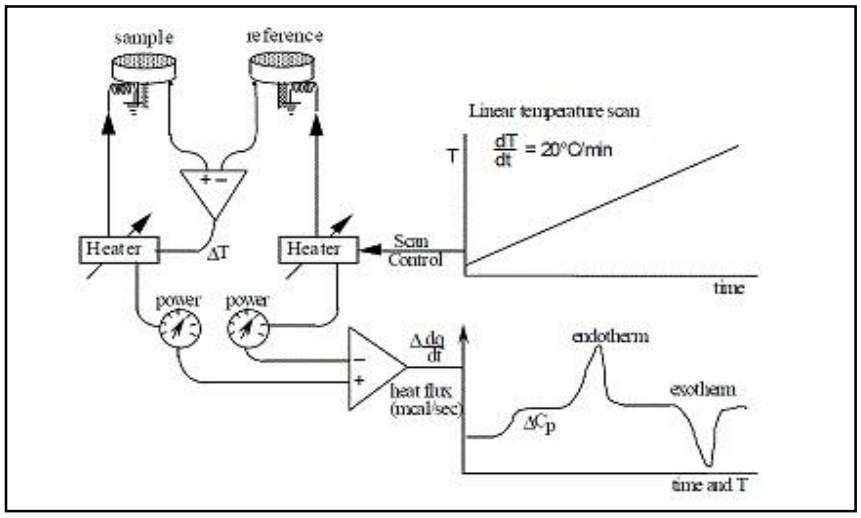

Figure 2.8: A schematic diagram of DSC and a DSC curve[14] [76].

[14] Two different conventions exist for the display of the heat flow curve: one shows endotherms in the downward direction, the other upward. The operator has a choice with most software packages [76].

2.6.2.1.2 Enthalpy

The enthalpy of a material is the energy required to heat the material to a given temperature [77]. The DSC curve is the graphical display of the heat flow (dH/dt) that flows to the sample. The enthalpy change is then an area under the DSC curve between two time limits [25].

$$\Delta H = \int_{t1}^{t2} \frac{dH}{dt} dt$$

(Eq. 2-12)

2.6.3 Thermal characterization of a geopolymer

The complex physical and chemical process involved in geopolymerization releases a great deal of chemical reaction heat [10]. Previous research on the thermal characterization of geopolymers have focused on the application of different thermoanalytical techniques [78-82] in order to obtain a good understanding of the geopolymerization process, with the most commonly used technique being calorimetry.

As was discussed previously (see Figure 2.5), geopolymerization is a multistep chemical reaction process involving dissolution, polymerization, and transformation (reorganization/crystallization). During the process, multiple heat flow peaks (exothermic peaks) are observed, which is what led Rahier et al. [83] to discover the first two steps of the process—dissolution and polymerization.

In the first stage of the reaction process, geopolymerization begins with the dissolution of the solid particles at the surface of the source material into silicate and aluminate monomers. This is the first exothermic reaction. The second exothermic reaction is observed in stage two, where the silicate and aluminate monomers polymerize into aluminosilicate oligomers, which immediately then polymerize into small geopolymeric fragments. The final exothermic peak, in stage three of the reaction, has two possible transformations: the formation of crystalline and the reorganization of the solid structure into a more thermodynamically stable state [59]. Although these stages are

described separately, they may occur simultaneously and can hardly be separated [51]. A schematic diagram relating the three exothermic peaks with their three stages in reaction time is shown in Figure 2.9.

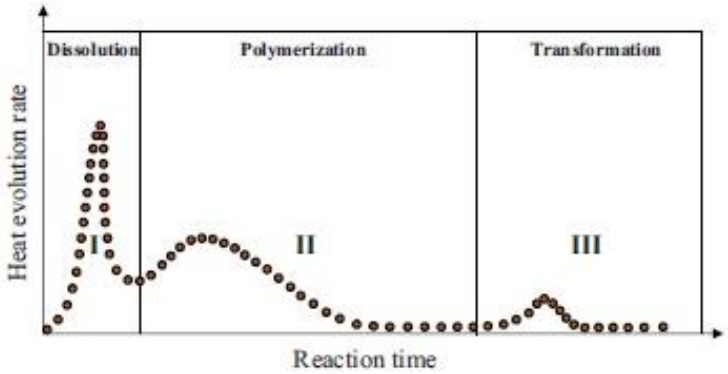

Figure 2.9: Schematic of the kinetics of geopolymer synthesis as determined by isothermal calorimetry [59].

Yao et al. [58] investigated the heat evolution of alkali-activated metakaolinite using a 3114/3236 TAM Air isothermal calorimeter. Figure 2.10 is the DSC curve of that reaction, showing that an exothermic peak (A) appears immediately after mixing metakaolinite with the alkaline solution. This indicates an intensive instance of absorption of the alkali solution on the surface of the metakaolinite particles, implying the attacking and breaking down of the Si-O and Al-O bonds on particle surfaces by the OH^- anions. The second exothermic peak (B) indicates a drastic breakdown of metakaolinite particles and the formation of alumina/silica-hydroxyl species and oligomers. As the products of destruction grow up, they polymerize into gels, becoming the main heat evolution peak (C), after which the freshly formed small gel transforms into a larger network and the process enters a thermally steady state.

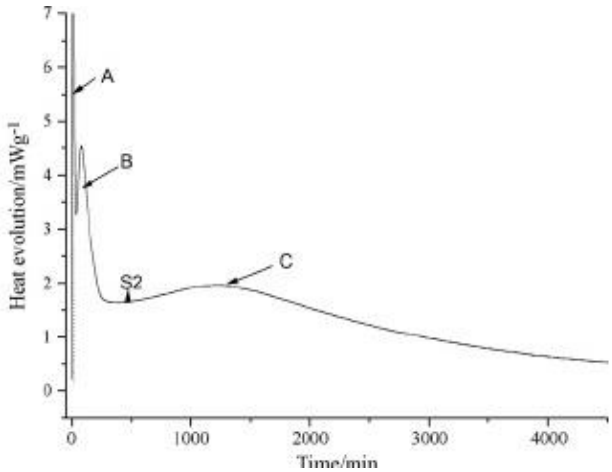

Figure 2.10: Calorimetric curves of metakaolinite activated by a 9 mol/LNaOH solution. Peak (A) indicates dissolution of the metakaolinite particles, peak (B) indicate polymerization, and peak (C) indicates Transformation. These corresponds to stage I,II,III of Figure 2.9 respectively [58].

By analyzing the heat evolution, calorimetry is one of the most effective techniques used in characterizing the reaction rate and reaction process of cementitious materials. The results acquired are usually used for [84]:

— Determination of the relationship between degree of reaction and physical properties.

— Elucidation of the mechanism of reaction.

The entire reaction process of geopolymerization has been observed in isothermal conduction calorimetry to be exothermic [82]. Hence, reaction enthalpy can be used to directly represent the extent of the reaction [85]. This then implies that the extent of geopolymerization of raw materials can be characterized by the heat evolution: more reaction heat released in the system indicates a higher level of geopolymerization and better mechanical properties in the final product. This is affirmed by Rahier et al. [24], illustrating the relationship between heat release data and the final mechanical strength of the geopolymeric products (Figure 2.11).

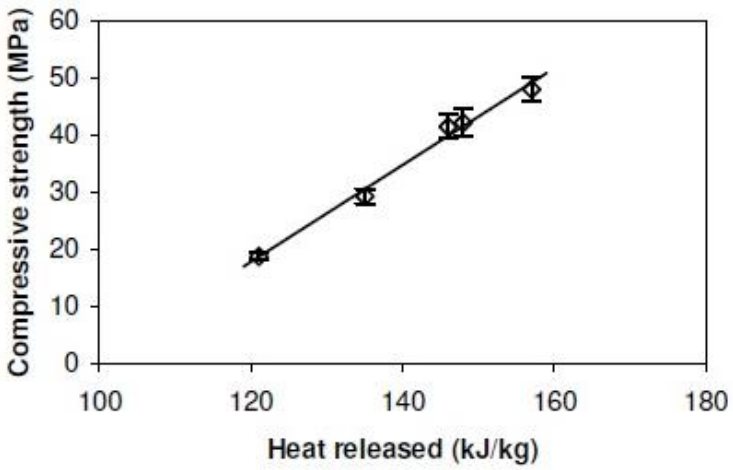

Figure 2.11: Relationship between total reaction enthalpy and product strength in geopolymers [24].

2.6.3.1 Factors affecting the geopolymerization process/heat evolution

There are numerous factors that affect the rate of heat evolution observed by calorimetry techniques during the geopolymerization process. But only those factors that are of concern to this thesis will be discussed. These include:

- Reaction temperature
- Concentration of chemical activator solution (MOH)
- Modulus of alkali silicate solution
- Addition of a retarder

Effect of reaction temperature

A moderate elevation of the reaction temperature is found to increase the compressive strength of a geopolymer [41, 58, 86]. At a low temperature, the rate of dissolution of raw materials and the rate of geopolymerization are slow. At a high[15] temperature, a large amount of Si^{4+} and Al^{4+} will form in the alkali solution and immediately polymerize into gels, disrupting further dissolution by covering the solid particle surface [58]. This results in a short heat evolution time, leading to low heat evolution. In addition, a high temperature could cause the loosing of water more rapidly due to an exothermic reaction, resulting in the formation of micro-cavities which cause an increase in porosity [87].

[15] The margin separating "low" and "high" temperatures is observed to be approximately 40-80°C [56].

Muñiz-Villarreal et al. [87] studied the effect of temperature on the extent of geopolymerization using Mettler Toledo DSC822E and found an optimum reaction temperature of 60^{o}C. At this temperature, the system releases more heat, which results in a higher extent of geopolymerization than is observed at other temperatures. (See Figure 2.12.) Similar observations have been made of synthetic geopolymer systems but with different optimum temperatures, such as 35^{o}C, 40^{o}C, etc. [58, 59, 88]. These results suggest that an optimum reaction temperature could increase the reaction rate and extent of the reaction of raw materials [58], and that this varies for a given geopolymeric material with a given activator.

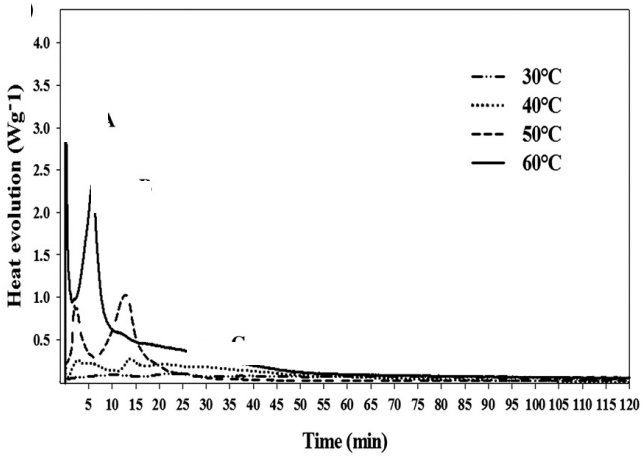

Figure 2.12: Calorimetric results at different curing temperatures showing 60^{O}C as the optimal temperature with the highest heat evolution. [87].

Effect of chemical activator

The concentration of MOH (M = Na^+ or K^+) plays a vital role on the mechanical properties of a geopolymer. Generally, a strong chemical activator is necessary to increase the dissolution of the aluminosilicate particles present in the raw material [2]. This implies that increasing an alkali concentration increases the reaction extent. Figure 2.13 shows that the alkali concentration also has a great influence on the initiation of the geopolymerization process. It is certain that the system tends to release more heat as the concentration of KOH increases, as investigated by Yao [58]. The increase in compressive strength/heat evolution that occurs as the chemical activator concentration increases is attributed to a high degree of silica and alumina dissolution [2]. This is attributed to

raise levels of M in the mixture, which plays an important role in charge balancing during the formation of the geopolymer. However, while M ions are beneficial for aluminosilicate leaching, an excessive concentration of MOH is undesirable in polymerization [58] as an excessive OH^- concentration will cause premature precipitation of aluminosilicate gel, resulting in a lower-strength geopolymer [2].

Different effects are associated with alkali cation types in geopolymerization. Yao et al. [58] observed more dissolution of aluminosilicate in a KOH solution, and concluded that it has a better activation efficiency than NaOH. This may be due to the high viscosity of the NaOH solution, which hinders the dissolution of alumina and silica species [2]. This is in line with the research carried out by Van Jaarsveld et al. [89], showing that K^+ increases the strength of geopolymeric materials.

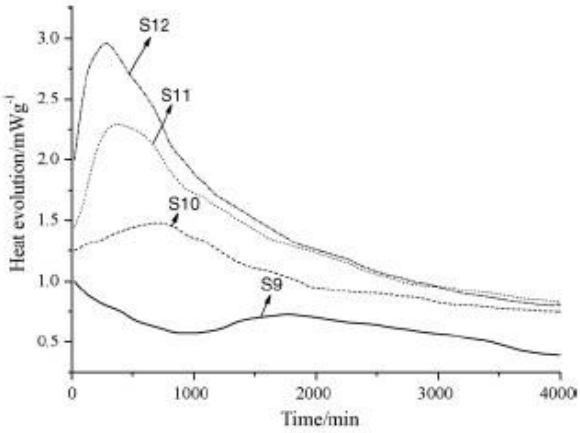

Figure 2.13: Effects of the concentration of a KOH solution on geopolymerization, from low (S9) to high (S12) concentration. S12 is the optimum concentration with the highest heat evolution [58].

Effect of modulus of alkali silicate solution

A geopolymerization reaction is observed best in the presence of an alkaline medium, and adding silicate can create another ionic composition with excellent bonding effects [90]. The inclusion of alkali silicate in an alkali solution provides higher silicate content, which can accelerate geopolymerization by inducing the polymerization of the leached products [58]. This increases the mechanical properties beyond what can be produced by a hydroxide activator alone [52]. The

modulus of the alkali silicate solution is vital in the reaction extent of solid materials. However, excess silicate in the system can reduce the heat evolution and the compressive strength of the geopolymer as excess silicate disrupts the evaporation of water and also hampers the formation of a three-dimensional aluminosilicate structure [2].

Studies by Yao et al. [58] and Duxson et al. [91] have shown that the reaction extent of the raw material increases with decreasing soluble silicon content at constant Na_2O/H_2O ratio[16]. Figure 2.14 shows an increase in heat evolution (reaction rate) correlating with a decrease in the modulus of a potassium silicate solution during stage one and stage two of the geopolymerization process.

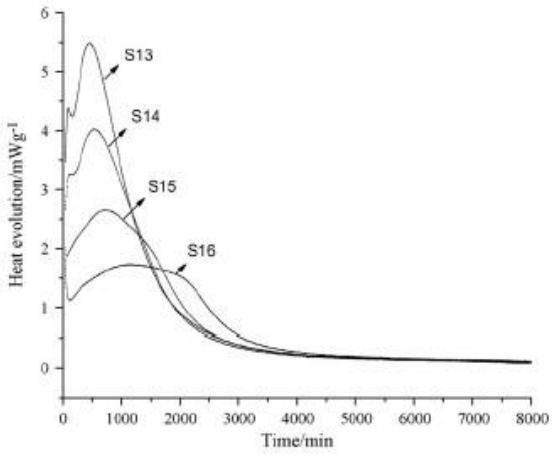

Figure 2.14: Effects of modulus of K-water glass on geopolymerization, from low (S13) to high (S16) modulus. S13 is the optimum modulus of K-water glass with the highest heat evolution. [58].

Effect of retarder

Retarders are used in geopolymer mix-designs to delay the setting time, especially during delays between mixing and casting. They normally reduce the solubility of hydrating components in the geopolymer matrix [47]. Sucrose is a widely used retarder; however, a high dosage may lead to flash setting.[17] (A detailed analysis on the effect of sucrose was outlined in Section 2.3.4.)

The inclusion of a retarder has been observed to have at least a comparable compressive strength to non-retarder mixtures [10, 22]. This can be observed in the heat evolution of the system as shown

[16] Na_2O/H_2O ratio means sodium oxide/water ratio

[17] Flash setting is a rapid development of rigidity in freshly mixed cementitious paste, mortar, or concrete.

in Figure 2.15. Although a retarder could reduce the heat release rate, the retarding effect is obvious as heat will continue to be released in the system for a prolonged time. This leads to a prolonged gelation time [10], which results in a better reaction extent than a non-retarder mixture.

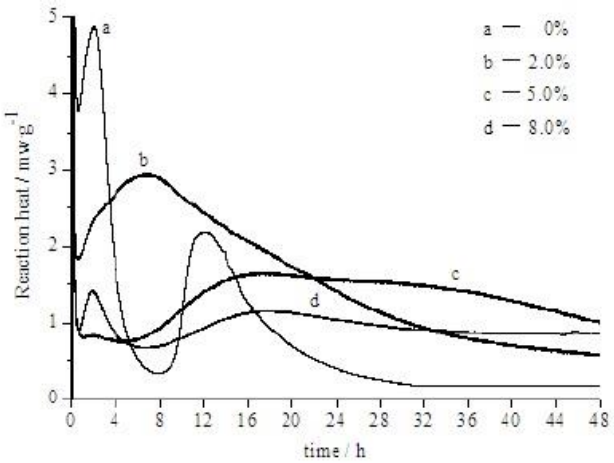

Figure 2.15: Effects of retarder dosage on heat evolution of different alkali activation systems with a) 0%, b) 2.0%, c) 5.0%, and d) 8.0% retarder dosage .The optimum dosage is 5.0% with heat evolution still observed in the system at 48 hours, which leads to better reaction extent and compressive strength. Flash setting was also observed at a dosage of 8.0%, with a small, early exothermic peak appearing at 1.8 hours [10].

3

MATERALS AND EXPERIMENTAL METHODS

3.1 Overview

This chapter presents a detailed overview of all the experimental methods used for the development of aplite-slag based geopolymer specimens. The specifications and properties of the materials used, as well as the mix-designs, are described. Furthermore, the test program and the test parameters used to examine and analyze the results are also explained.

3.2 Materials

The following materials have been used in this thesis for the geopolymeric formation.

3.2.1 Slag

The slag used to produce the aplite-slag based geopolymer was a commercial ground granulated blast furnace slag (GGBFS) with the product name “Merit 5000,” supplied by the Merit 5000 company of Sweden. The GGBFS was used as an additive to compensate the low aluminum content of the aplite rock.

Table 3-1 shows the chemical composition of the GGBFS used, as provided by the supplier.

Table 3-1: Chemical composition of GGBFS.

Compound	Chemical Content (weight %)
SiO_2	34.0
Al_2O_3	13.0
CaO	31.0
MgO	17.0
Na_2O	0.9
TiO_2	2.4
MnO	0.6
S^{-2}	1.1
LOI	-

Note: LOI: Loss on ignition[18]

For a ground granulated slag to be a successful slag binder material, its basicity coefficient should be greater than 1 (K_b>1). The basicity of a slag material is described as the ratio of the total basic content to the total acidic content, as shown in Equation 3-1[19] [92], and it is divided into three groups:

— Acidic slag (K_b < 1)
— Neutral slag (K_b = 1)
— Basic slag (K_b > 1)

Among the three groups, basic slag has been observed to be more active during alkaline activation, resulting in better mechanical strength. Acidic slag is more difficult to activate, leading to poor mechanical strength [93].

[18] Loss on ignition is a test used in mineral analysis in which a sample is strongly heated at a specific temperature, allowing volatile substances to escape until its mass ceases to change.
[19] The weight percentage of Fe_2O_3 and K_2O is zero (0). Hence, it is not included in the table above.

$$K_b = \frac{w_{CaO} + w_{MgO} + w_{Fe_2O_3} + w_{K_2O} + w_{Na_2O}}{w_{SiO_2} + w_{Al_2O_3}}$$

(Eq 3-1)

Furthermore, its CaO/SiO_2 and Al_2O_3/SiO_2 weight percentage ratios should be from 0.5 to 2.0 and from 0.1 to 0.6, respectively [94]. In addition, the hydration modulus (HM) should exceed 1.4 for good hydration properties, using Equation 3-2 [95].

$$HM = \frac{w_{CaO} + w_{MgO} + w_{Al_2O_3}}{w_{SiO_2}}$$

(Eq 3-2)

The GGBFS used in this thesis complies with all of the above requirements, with the basicity coefficient (K_b) of 1.04, CaO/SiO_2 weight percentage ratio of 0.91, Al_2O_3/SiO_2 weight percentage ratio of 0.38, and the HM of 1.79.

3.2.2 Aplite

In this work, aplite rock was used as a starting material for geopolymerization. It is rich in sodium (Na) and also contains a large amount of SiO_2 and Al_2O_3. The samples for this study came from Finnvolldalen, Namskogan, Norway, where aplite is found in abundance. It was used without any processing other than grinding.

Table 3-2 shows the chemical composition of the ground aplite.

Table 3-2: Chemical composition of aplite rock.

Compound	Chemical content (Weight %)
SiO_2	82.80
Al_2O_3	9.04
Fe_2O_3	0.75
CaO	0.82
MgO	0.10
Na_2O	2.72
K_2O	3.11
Cr_2O_3	<0.01
TiO_2	0.04
MnO	0.02
P_2O_5	0.005
SrO	0.02
BaO	<0.01
LOI	0.29

Khalifeh et al. [23] has recently studied the utilization of this aplite rock as a source material for geopolymerization, and with the use of X-ray power diffraction (XRD), quartz has been found to be the most abundant of its crystalline phases, while albite and muscovite are found as minor crystalline phases.

3.2.3 Microsilica

Microsilica (also known as silica fume) is a mineral admixture made of very fine, solid, glassy spheres of amorphous silicon dioxoide (SiO_2). It is a by-product of the industrial manufacturing of silicon metal or ferrosilicon alloy [96].

Microsilica is mainly used as a pozzolanic[20] material for high strength development and reduction of permeability in concrete [23].

For this thesis, microsilica Grade 955 was supplied by the Elkem Company of Oslo, Norway. It is composed of ultra-fine amorphous spheres of silicon dioxide, and it was used as a microfiller to make a high-performance geopolymer [23] by decreasing average pore size in the geopolymer paste [96]. Its Chemical composition is given in Table 3-3.

Table 3-3: Chemical composition of microsilica.

Compound	**Chemical content (Weight %)**
SiO_2	95.5
Al_2O_3	0.7
Fe_2O_3	0.3
CaO	0.4
MgO	0.5
Na_2O	0.4
K_2O	1.0
C	1.0
LOI	2.0

3.2.4 Alkaline activators

The activator was a solution containing a combination of Potassium silicate (K_2SiO_3) and Potassium hydroxide (KOH).

The Potassium silicate solution was supplied by Univ AS, Norway. Its chemical content was reported to contain 38 weight % of K_2SiO_3 and 62 weight % of H_2O.

[20] Pozzolans are a class of siliceous and aluminous materials which normally react with calcium hydroxide to form additional cementitious material.

Potassium hydroxide pellets with 99% purity were supplied by Merck KGaA of Germany. The potassium solution was then prepared by dissolving Potassium hydroxide pellets in deionized water, obtaining a low alkaline solution of a 4M KOH concentration in order to lower the risk of hazard, as a higher concentration of this substance is classified as corrosive [23].

3.3 Sample preparation

Prior to the preparation of the aplite-slag based geopolymer slurry, a 4M concentration of KOH solutions was prepared at least 24 hours before usage, to ensure all the components were homogenously mixed [23].

To prepare the slurries, the solid phase components (aplite, GGBFS, microsilica) were accurately measured using a Mettler Toledo mass balance. Thereafter, they were mixed together at dry conditions using a woven-wire mesh sieve which is used for all types of laboratory sampling and particle size analysis, to check for larger aggregates. The liquid phase components (KOH, k-silicate) were also accurately measured using the same Mettler Toledo mass balance. The Mettler Toledo mass balance used for this experiment is shown in Figure 3.1.

Figure 3-1: The Mettler Toledo mass balance (with an accuracy of -/+ 0.01 g).

The mixing of the solid phase and the liquid phase was carried out using an OFITE Model 20 Constant Speed Blender (see Figure 3.2), which is used for oil well cement testing. The liquid phase and retarder (sucrose) were mixed for 20 seconds. Afterwards, the solid phase was gradually added to the liquid phase during the period of 15 seconds at 4000 RPM and 35 seconds at 12000

RPM in accordance with API 10B-2 standards [97]. Deionized water was used in all the experiments to provide the medium for the dissolution of aluminosilicates, the transfer of various ions, the hydrolysis of Si^{4+} and Al^{3+} compounds, and the polycondensation of different silicate and aluminate silicate hydroxyl species. Table 3-4 shows the mix-designs of the geopolymeric slurries.

Figure 3.2: OFITE model 20 constant speed blender.

Table 3-4: Mix-designs of the geopolymeric slurries.

Sample	Alkali solution/ Alkali silicate solution by weight	Deionized water/ Activator ratio by weight	Solid/ Total solid fraction by weight				Liquid/ solid ratio by weight
			Sucrose	Micro-silica	GGBFS	Aplite	
1	0.431	0.097	-	-	0.303	0.697	0.514
2	0.431	0.097	0.012	-	0.299	0.689	0.507
3	0.431	0.097	0.018	-	0.298	0.685	0.504
4	0.431	0.097	0.012	0.015	0.294	0.678	0.500
5	0.431	0.097	0.017	0.029	0.289	0.665	0.490
6	0.454	0.097	0.012	0.015	0.294	0.678	0.500
7	0.454	0.097	0.017	0.029	0.289	0.665	0.490

The mixture was immediately poured into an atmospheric consistometer slurry cup for conditioning. Atmospheric consistometers are designed for low temperature cement systems, but have also found an application in the conditioning of geopolymer slurries before testing. The main purpose of using an atmospheric consistometer for geopolymer slurries at this stage is for proper homogenous mixture of the phases. All the mix-designs mixtures used in this experiment were conditioned for 20 minutes at atmospheric pressure according to API 10B-2 standards [97] prior to analyzing their thermal properties. The atmospheric consistometer used in this experiment is shown below in Figure 3.3.

Figure 3.3: Atmospheric consistometer.

3.4 Analytical method

To study the thermal properties of the geopolymer slurries, the DSC heat evolution technique was used. DSC has been shown to be a useful technique in studying the hydration of cementitious materials, especially isothermal calorimetry, which has the advantage of testing a material at a specific temperature and has been used by many researchers in the study of green cementitious materials [10, 58, 98, 99]. Basically, isothermal calorimetry is used for investigating a major thermal peak that occurs during the hydration process of a cementitious material.

For this experiment, a Mettler Toledo Differential Scanning Calorimeter was used in accordance with ASTM D3418-15 standards [100]. For accuracy and repeatability of data, the calorimeter was calibrated and checked under the conditions of use in accordance with ASTM E968-02 standards

[101]. The calibration was carried out by measuring the temperature and the physical properties, in conjunction with measured signal (heat flow, peaks area), of a standard specimen[21] for which these quantities are known [25]. The result of the calibration is given in Appendix B.

The conditioned geopolymeric slurries were loaded into a 40µl standard aluminum crucible with lid, and then weighed before and after the experiment using a Mettler Toledo mass balance to determine a possible mass loss of volatile substance from the sample. Figure 3.4 shows the aluminum crucible and lid used in this experiment.

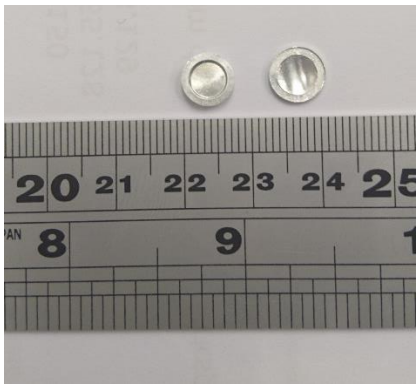

Figure 3.4: 40µl standard aluminum crucible with lid.

The lid of the crucible was pierced with a single hole of about 50µm, at the center to avoid internal pressure buildup in the crucible during the experiment. Thereafter, the crucible with the sample inside was hermetically sealed and loaded into the calorimeter sample furnace chamber, while the reference furnace chamber was loaded with an empty aluminum crucible. The calorimeter and the furnace are shown in Figure 3.5 below.

The advantages and limitations of using this DSC technique in characterizing geopolymer materials can be found in Appendix C.

[21] In this case, zinc was used with the following standard properties:
T_F: 419.6°C ΔH_f: 107.5 J/g

Figure 3.5: Differential Scanning Calorimetry: (a) the calorimeter; (b) the reference and the sample furnace chamber; (c) the furnace chamber with the furnace lid on.

The calorimetry test on the slurries was divided into two groups:

In group one, the test was run with the calorimeter set at two different segments: dynamic and isothermal segment, with a starting temperature of 25^{o}C. The dynamic segment was used to ramp-up the temperature of the slurries from 25^{o}C to 50^{o}C at a ramp-up rate of 1.8^{o}C/min and thereafter kept isothermally at 50^{o}C for 16 hours using the isothermal segment of the DSC.

In group two, the test was run for 16 hours with only the isothermal segment of the calorimeter set at a temperature of 25^{o}C.

The heat release of the system was then recorded. However, the recorded curves could not be directly compared because different amounts of samples were used and the larger sample sizes produced broader effects. To overcome this, the recorded curves were normalized to their sample sizes, allowing the recorded curves to then be compared.

4

RESULTS AND DISCUSSION

This chapter will present the results and discussion of the effect of the different parameters on the thermal properties of the geopolymer.

It is worth reminding that the mix-designs used in this work possess different admixture contents, resulting in different thermal effects. Readers can refer to Table 3-4 in Section 3.3 for the contents of the different mix-designs used.

4.1 Geopolymerization of KOH/ K_2SiO_3 activated aplite-slag slurries

Figure 4.1 shows the heat evolution curves through 16 hours for KOH/ K_2SiO_3 activated slurries (upper curve segment). The experiment was carried out by ramping up the temperature of the slurries from 25°C to 50°C at a ramp-up rate of 1.8°C/min, and thereafter kept isothermally at 50°C for 16 hours (lower curve segment). The calorimetric response shows at least two exothermic peaks—an early peak at dissolution and an accelerated peak (polymerization) appearing later.

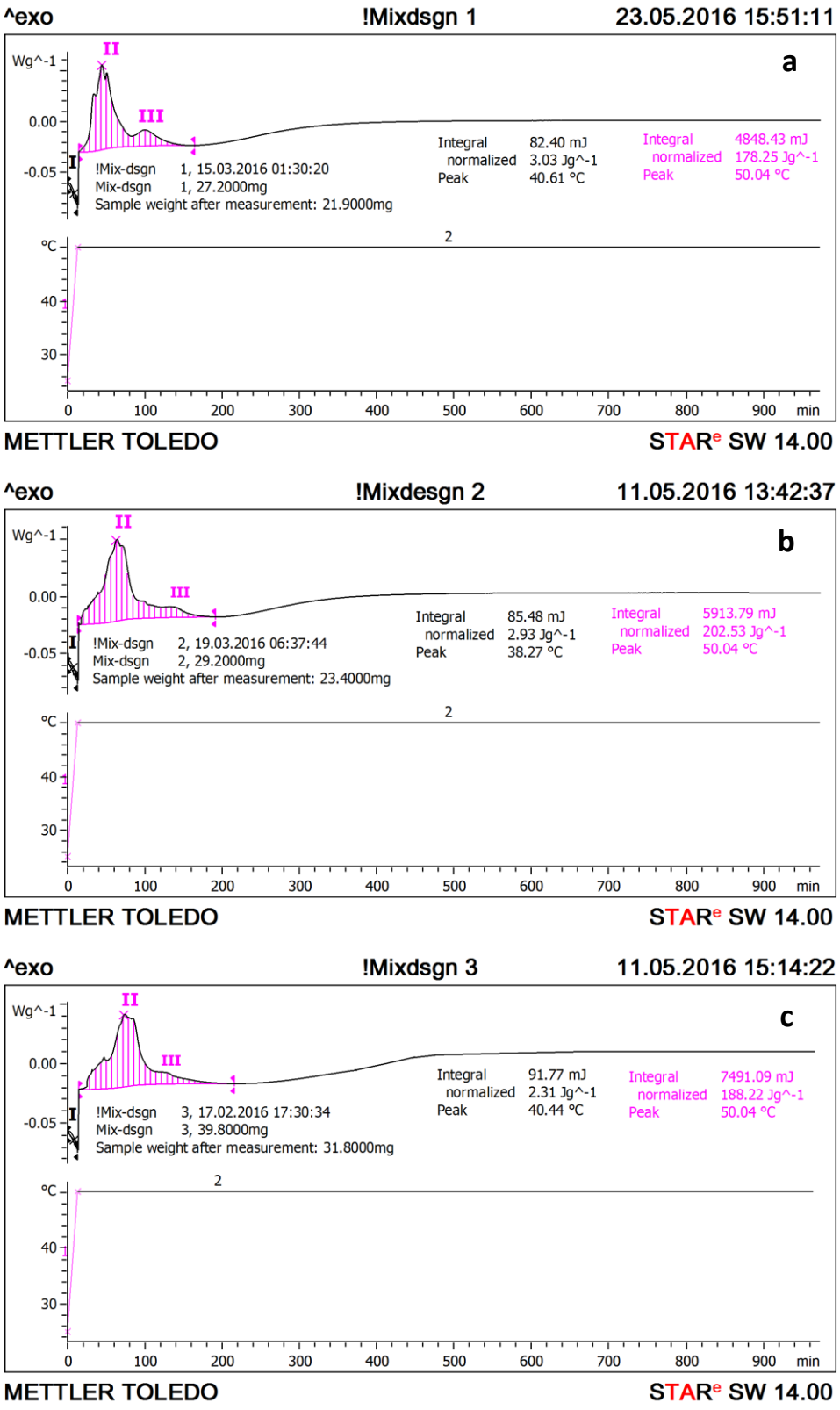

Fig 4.1: Non-isothermal calorimetry curves for: a) Mix-design #1; b) Mix-design #2; and c) Mix-design #3.

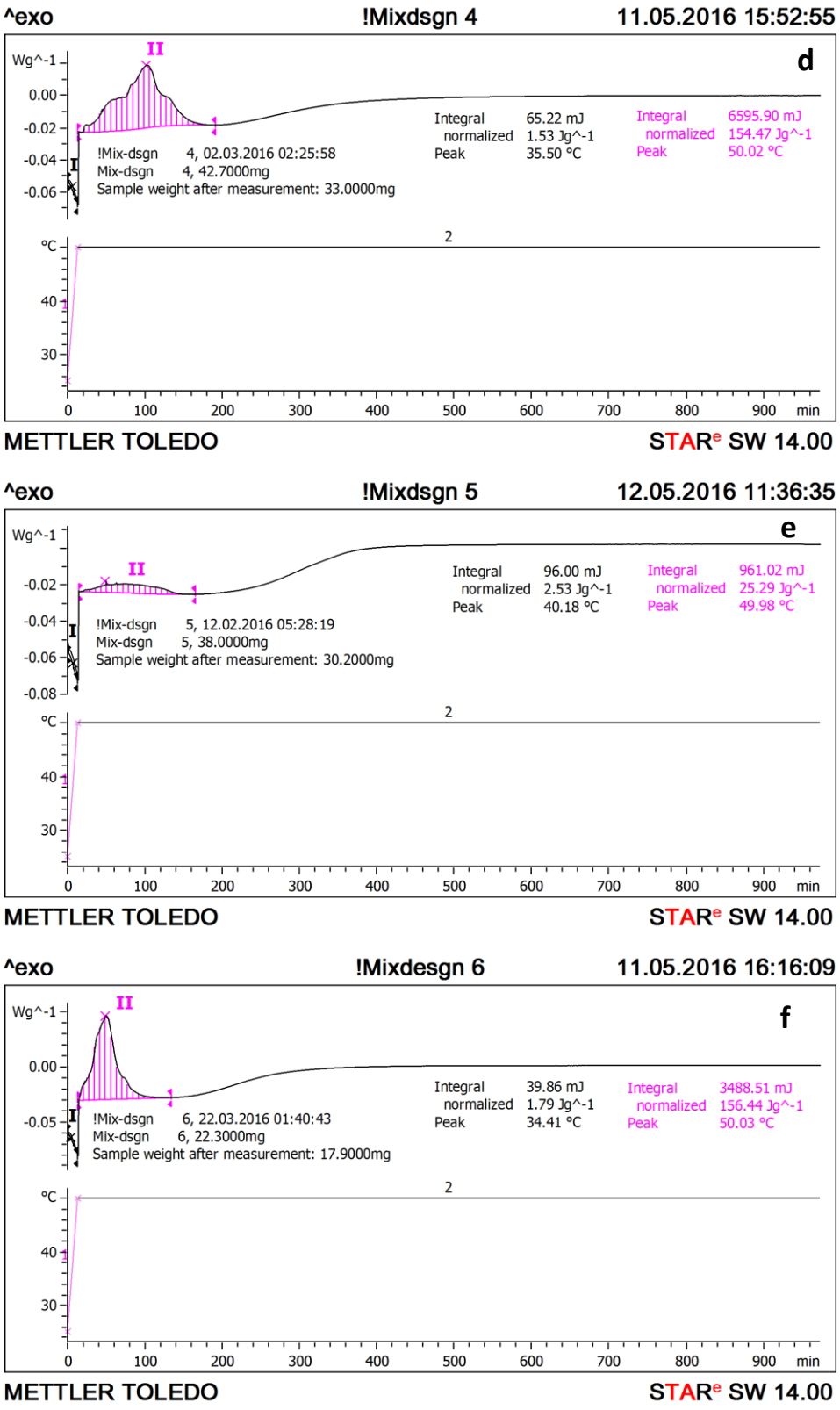

Fig 4.1: Non-isothermal calorimetry curves for: d) Mix-design #4; e) Mix-design #5; and f) Mix-design #6.

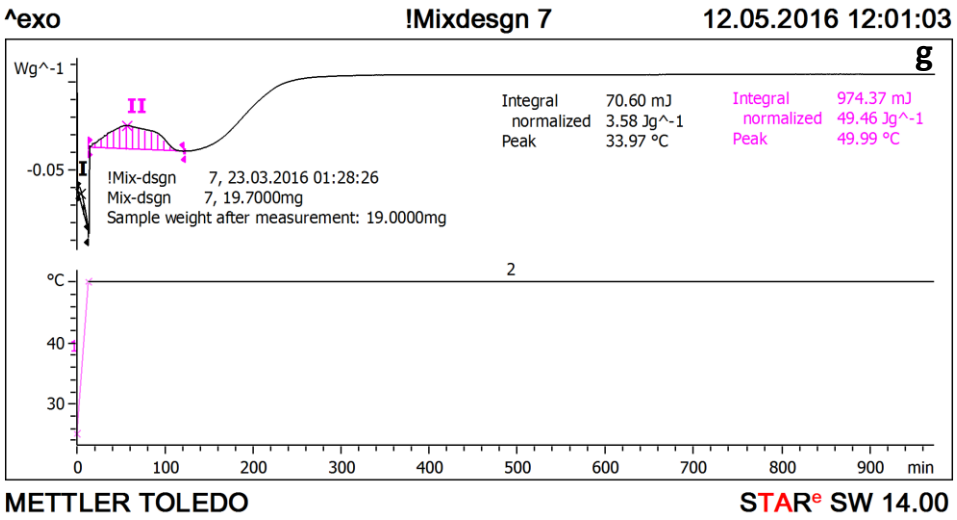

Fig 4.1: Non-isothermal calorimetry curves for: g) Mix-design #7.

The very early, narrow exothermic peak I appearing during the temperature ramp-up corresponds to the absorption of the alkali solution on the surface of the aplite-slag particle and the beginning of the dissolution of the aplite-slag particles. This indicates that the OH^- anions are attacking the Al-O and Si-O bonds on the particle surfaces, breaking them into the aqueous solution, thus enabling the formation of alumino-silicate units and their complexation with the alkali ions [58, 98]. This early exothermic peak is observed in all the mix-designs (see Figure 4.1a-g) used in this experiment, implying an absorption of the alkali solution on the surfaces of the aplite-slag particles in all the mix-designs. It is also worth noting that at the beginning of the dynamic program, there was a baseline change which appeared to be endothermic (see Appendix B). This is a normal occurrence caused by differences in the heat capacities of the sample and the reference pan. Since the heat capacity of a sample is directly related to its weight, an initial endothermic shift (known as an endothermic start-up hook) indicates that the reference pan is too light to offset the sample [102]. Hence, the first few seconds are not taken into account.

After peak I, a second exothermic peak II appears. This indicates a further and drastic break down of the aplite-slag particles, as well as the formation of silica/alumina hydroxyl species and oligomers, such as $Al(OH)_4^-$, $OSi(OH)_3^-$, and $(OH)_3–Si–O–Al–(OH)_3$ [58]. When the concentrations of the silica/alumina hydroxyl monomers and other small, dissolved species reach

a critical level that exceeds saturation in the alkaline environment, then polymerization of the silicate and aluminate monomers into aluminosilicate oligomers occurs, thus becoming the dominant reaction. However, due to the high concentration OH^- in the aqueous phase, the freshly formed species are further broken down as intermediates [58] which immediately polymerize into small geopolymeric fragments. The disaggregated products in the aqueous phase will accumulate to form a coagulated structure which is thermodynamically metastable and will transform into amorphous or semi-crystallized phases [88]. This second peak of polymerization is exothermic and becomes the main contribution of the system's heat evolution.

The amplitude of the heat release at peak II varies significantly in each system as the concentration of the admixture (sucrose and microsilica) is changed. The maximum heat release rate decreases with increasing soluble silicon content. This is attributed to low polymerization taking place between Si and Al species in the system. Further discussion on this point will be presented later.

A third exothermic peak III is clearly observed in a system without a retarder (mix-design #1—neat paste). As seen in Figure 4.1, Peak III gradually decreases with an increase in the retarder concentration, indicating that peak III is probably caused by the initial reorganization among the polymer precursors [59]. This may be attributed to the rapid polymerization of the neat paste, allowing no time for the reorganization of the geopolymer precursors during the gelation process [88]. But with the addition of a retarder, the intensity of peak III decreases, implying gelation and reorganization of the geopolymer precursor happen simultaneously, due to the prolonged polymerization time.

After about 500 minutes, the geopolymerization process goes into a thermally stable stage, during which the reorganization process continues and the freshly formed, small geopolymeric fragment gels are transformed into larger networks [58], resulting in the formation of a three-dimensional aluminosilicate network.

A possible loss of mass in the samples is observed by back-weighing the samples after the measurements. (See Table 4.1.) This mass loss indicates the sample loses a volatile substance, which could possibly be water, as proposed in the literature given in Section 2.5.

Some sharp, small peaks which may be related to crystallized phases were also detected, especially in the neat paste mix-design between 40 and 80 minutes of the reaction time. These peaks may indicate a specific crystallization event in the gel system. Many authors have observed the

formation of phases described as semi-crystalline [23, 51], especially in a system with a slightly low alkali concentration and little or no soluble silicon present in the alkali medium.

The crystalline phases are usually zeolite, which favors its formation at a higher reaction temperature [51, 59]. This can be observed in Figure 4.2, where small, sharp peaks are recorded in mix-design #1, measured non-isothermally at 50°C, while there are no small, sharp peaks in mix-design #1, measured isothermally at 25°C.

It is worth noting that the detected small, sharp peaks could be attributed to crystalline phases, yet this is only **"Hypothesis"** and further work and experiments must be done to confirm that the peaks are actually crystalline phases.

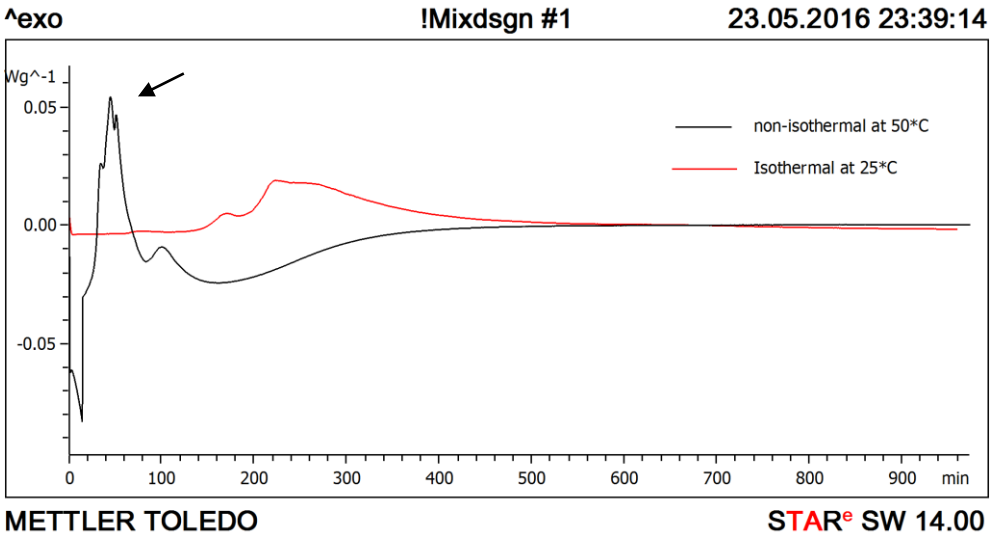

Fig 4.2: Effect of temperature on formation of crystalline phases where small, sharp peaks which may indicate a specific crystallization event dictated in the mix-design #1 measured non-isothermally at 50°C and no small sharp peaks dictated in the mix-design #1 measured isothermally at 25°C.

Figure 4.3 shows the results obtained when the geopolymeric slurries were subjected to only isothermal measurement using the isothermal segment of the DSC for 16 hours at 25°C. The purpose of this experiment was to determine the geopolymerization process of the geopolymer slurries at 25°C, then compute and compare the total heat evolution between the slurries measured at 25°C and 50°C in order to determine optimum curing temperature.

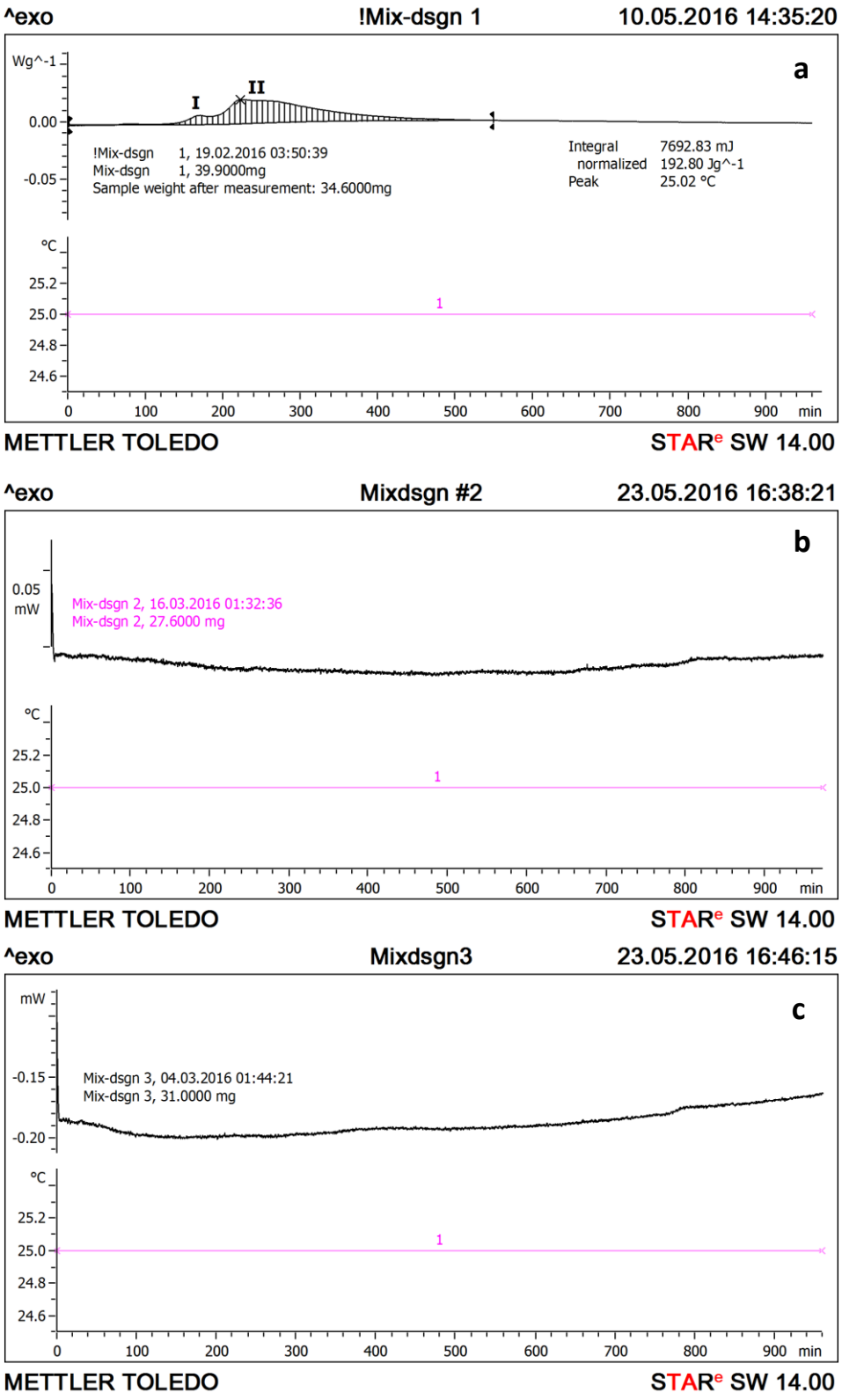

Fig 4.3: Isothermal calorimetry response at 25ºC for: a) Mix-design #1 with broad exothermic peak, b) Mix-design #2 with no calorimetry response, and c) Mix-design #3 with no calorimetry response.

Apart from the neat paste (mix-design #1) which shows a broad exothermic peak, indicating a curing reaction, the rest of the mix-design shows no indication of the geopolymerization process. This implies that the sensitivity of the DSC is too low to measure certain effects [103] during the geopolymerization process.

Because of this limitation, only in mix-design #1 will the optimum temperature be determined.

4.2 Determining the accumulative heat release

The amount of polymerization heat released as a function of time for all the mix-designs was calculated using Equation 2-12 To determine the accumulative heat release up to a certain time *t*, the area between an integral horizontal baseline and the DSC peak between time t_1 (the start point of the polymerization) and *t*, with *t* varying between t_1 and t_2 (the end point of the polymerization) was integrated.

By using Equation 2-12, the accumulative heat release for all *t* between t_1 and t_2 can be represented as:

$$\Delta H_{t1-t} = \int_{t1}^{t} \frac{dH}{dt} dt$$

(Eq. 4-1)

When *t* equals t_2, the total heat of polymerization was obtained as:

$$\Delta H = \int_{t1}^{t2} \frac{dH}{dt} dt$$

(Eq. 4-2)

The amount of heat released was calculated at 10-minute intervals and the integration was performed using the STARe evaluation software.

The accumulative heat released by the systems is summarized in Table 4.1. The total heat released in each case ranges from 27.82 J/g to 205.5 J/g for systems measured using both the dynamic and isothermal measurements, and 192.8 J/g for systems measured using only isothermal measurements

at 25ºC. For mix-design #1, a slight increase in heat release was observed for the system measured isothermally at 25ºC than that measured by ramping-up the temperature to 50ºC using both dynamic and isothermal measurement. This implies that a slow initial dissolution of the solid particle at 25ºC (this slow dissolution can be observed in Figure 4.3a where there seems to be an induction period from the beginning of the measurement up to about 100 minutes) resulted in higher heat released due to a better reaction extent of the solid particles. The same phenomenon, where a slow reaction at a low temperature resulted in higher heat released, was also observed in sodium hydroxide activation of metakaolin by Zuhua Zhang et al. [59].

Table 4-1: Heat released response parameters of the activated mixtures.

Sample	Magnitude of peak (mW/g) Peak II	Time to peak (min)	Accumulative heat release at 960 min (J/g)	Sample mass loss (mg)
1	82.83	43.07	181.3	5.30
2	71.26	63.46	205.5	5.80
3	60.81	73.29	190.5	8.00
4	39.03	101.2	156.0	9.70
5	6.22	49.11	27.82	7.80
6	76.29	49.87	158.2	4.40
7	13.21	57.42	53.04	0.70
Mix-design #1 measured isothermally at 25ºC				
1	21.36	222.1	192.8	5.30

The optimal accumulative heat release (see Figure 4.4) was obtained in mix-design #2 where 0.012 Solid/ Total solid fraction by weight (1.2% of solid phase) of sucrose was used as a retarder. The variation in total released heat within the mix-designs is mainly due to differences in the dissolution extent of the solid particles and the difference in the polymerization reaction, which is as a function of the Si/Al ratio [88].

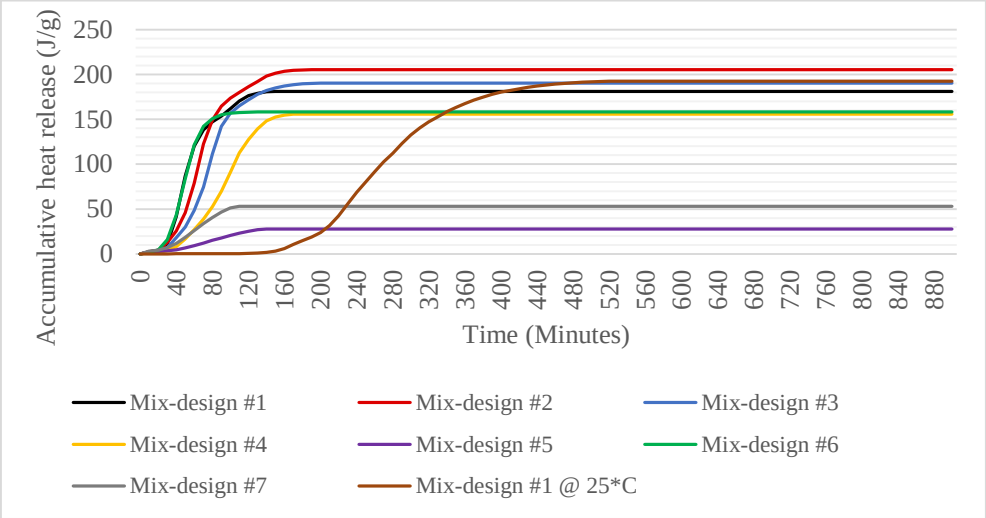

Fig 4.4: Accumulative heat released for systems measured non-isothermally at 50ºC and for systems measured isothermally at 25ºC.

4.3 Influence of retarder dosage on geopolymerization

The influence of the retarder dosage on the heat evolution of different alkali-activated geopolymeric slurries is presented in Figure 4.5 and Figure 4.6. It is clearly shown that the inclusion of a certain amount of sucrose could improve the heat evolution, which would result in better mechanical properties of geopolymers (see Figure 2.11 in Section 2.6.3 for the correlation between heat evolution and compressive strength).

The gelation time (polymerization) was much affected by the inclusion of sucrose in the mixture. The second exothermic peak of the geopolymeric slurry without a sucrose addition (mix-design #1) appears at 43.07 minutes with an 82.83 mW/g reaction heat. The heat release rate then decreases sharply until 164 minutes.

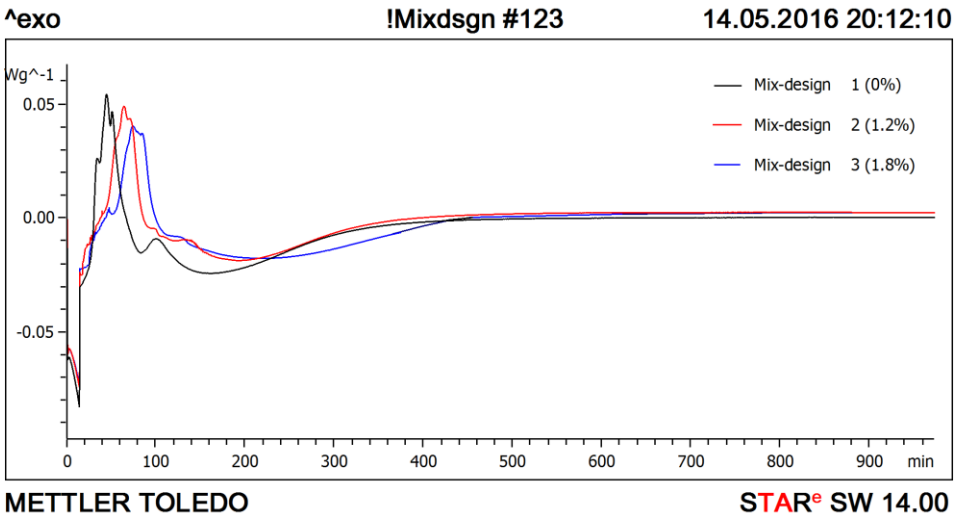

Fig 4.5: Effect of retarder dosage on the heat release rate of different alkali-activated aplite-slag based geopolymers.

Sucrose dosage may reduce the heat release rate. This is observed when the dosage is 1.2% of the solid phase (mix-design #2). The exothermic peak intensity of the system decreases, resulting in a 71.26 mW/g reaction heat, but the retarding effect is noticeable by the time shift where the second exothermic peak appears at 63.46 minutes. Heat release continues in the system until 191.2 minutes, resulting in a higher accumulative heat release than the non-sucrose mixture. This phenomenon is due to the absorption of sugar acid on the solid particle surfaces, which results in prolonged and better dissolution, leading to an increase in the concentration of several geopolymer precursors (Ca, Si, and Al) [22].

When the dosage of sucrose was 1.8% of the solid phase (mix-design #3), the second exothermic peak appears much later at 73.29 minutes, but with a much smaller reaction heat peak of 60.81mW/g. Although there was still heat release in the system until 216.1 minutes, the accumulative heat release was lower than that of mix-design #2. The explanation of this phenomena is that although the addition of sucrose promotes the concentration of several geopolymer precursors, sucrose also combines with Fe, Al, and Ca in the mixture to form insoluble metal organic complexes which disrupt dissolution and polycondensation [22]. Hence, a higher concentration of sucrose will lead to a significant reduction in the heat evolution and the mechanical properties of the material.

As shown in Figure 4.6a, the non-sucrose mixture has a gelation time of 43.07 minutes. The addition of sucrose as admixture delays the gelation time by 20.39 minutes and 29.32 minutes for 1.2% and 1.8% sucrose addition respectively. The 1.2% addition of sucrose in the aplite-slag based geopolymer presents the encouraging result of a significant increase in the accumulative heat release (see Figure 4.6b), which implies a better compressive strength for the geopolymer material.

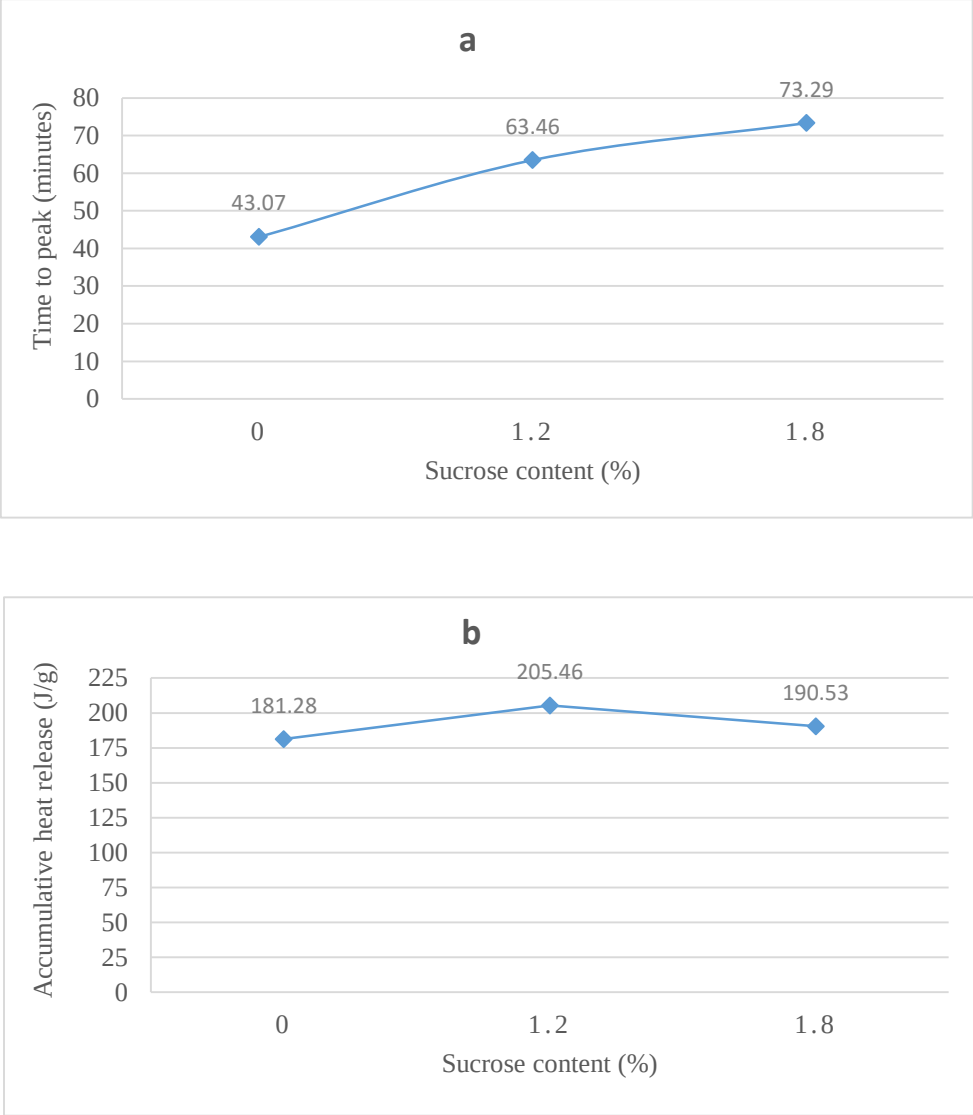

Fig 4.6: Relationship between sucrose content and: (a) time to peak (gelation time), and (b) accumulative heat release.

4.4 Influence of soluble silicate content on geopolymerization

As shown in Figure 4.7, the reaction rate decreases with an increasing silicate content (K_2SiO_3 + SiO_2). When microsilica (SiO_2) was added to the mixture, the solid silicate dissolved first from the solid source into the aqueous solution by reacting with the alkali solution (in this case KOH) and water already present in the aqueous solution. This produced potassium orthosilicate, potassium tetrasilicate, and water, which led to excess silicate being released into the geopolymer gel. The excess silicate in the geopolymer system reduces its accumulative heat release, resulting in compressive strength reduction, since excess silicate disrupts water evaporation and also hinders the formation of the three-dimensional gel structure of an aluminosilicate geopolymer [2].

Table 4-2: Mixture composition of the alkali activator and microsilica.

Sample	4M KOH (g)	K-silicate (K_2SiO_3) (g)	Microsilica (SiO_2) (g)	(K_2SiO_3 + SiO_2) (g)
1	93	216	-	216
4	93	216	10	226
5	93	216	20	236
6	96.5	212.5	10	222.5
7	96.5	212.5	20	232.5

Mix-design #4 and mix-design #6 are similar, with 0.015 Solid/ Total solid fraction by weight (1.5% of solid phase) of microsilica used as admixture to increase the silicate content. The only difference between the two mix-designs is the variation in K_2SiO_3 and KOH content. A 3.76% increase in KOH content and 1.62% decrease in K_2SiO_3 from mix-design #4 resulted in mix-design #6, with a rapid increase in the heat release rate and also an increase in accumulative heat release.

Mix-design #5 and mix-design #7 follow the same trend with 0.029 Solid/ Total solid fraction by weight (2.9% of solid phase) of microsilica and a variation in K_2SiO_3 and KOH content. Also, a 3.76% increase in KOH content and 1.62% decrease in K_2SiO_3 from mix-design #5 resulted in mix-design #7, with an increase in the heat release rate and also a rapid increase in accumulative heat release.

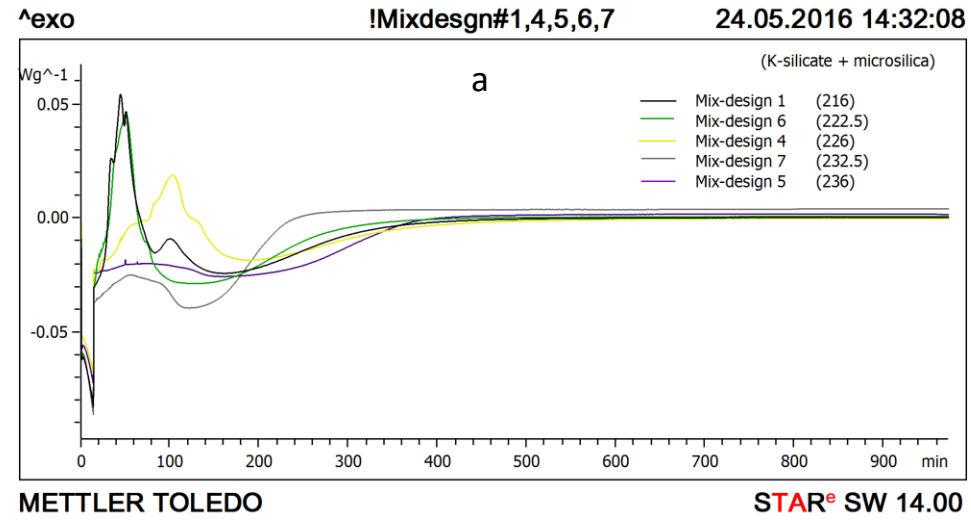

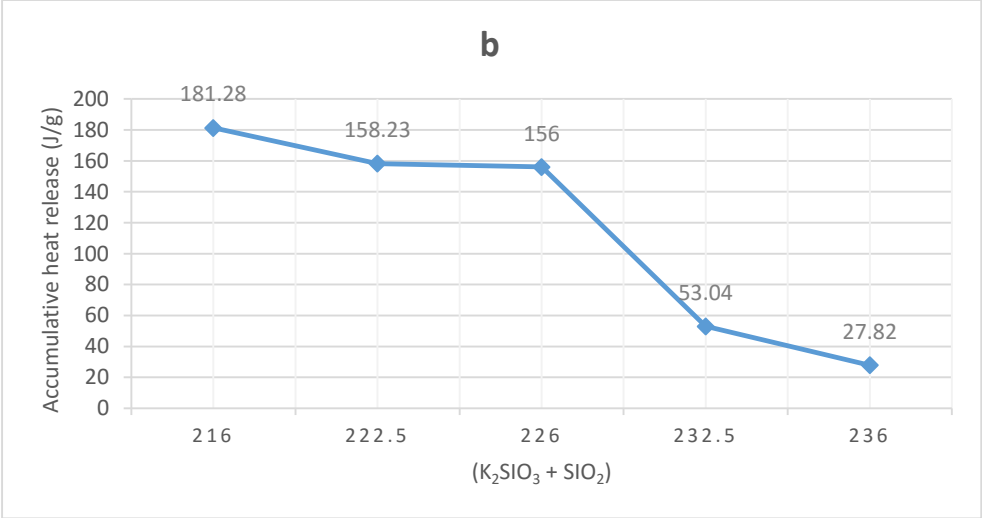

Fig 4.7: Relationship between silicate content and: a) the heat release rate and b) the accumulative heat release.

This result was caused by the change in the alkaline activator content, which affects different factors such as K^+ ions content, water content, and silicon species content. These factors have a major influence on the geopolymerization process, the heat evolution, and the resulting geopolymer compressive strength. The above result has shown that an increase in the alkali activator content (in this case KOH) will result in an increase in the hydroxyl ions (OH^-) content, which acts as a catalyst for the dissolution of aluminosilicate species from the source material. There will also be

an increase in the K^+ ions, which plays an important role in geopolymer formation by acting as charge balancing ions [2].

The variation of the total heat evolution implies that the reaction extent of the raw material increases with decreasing soluble silicon content at a constant K_2O/H_2O ratio, which is consistent with the results found by Yao et al. [58].

4.5 Influence of reaction temperature on geopolymerization

As mentioned earlier in Section 4.1, only mix-design #1 showed broad exothermic peaks when subjected to only isothermal measurement using the isothermal segment of the DSC for 16 hours at 25^{o}C. Therefore, only mix-design #1 will be used to analyze the influence of reaction temperature on geopolymerization.

As the temperature increases from 25^{o}C to 50^{o}C (as shown in Figure 4.8), the reaction rate (heat release rate) increases and the reaction time (gelation time) decreases. The accumulative heat release over 16 hours for systems at 25^{o}C and 50^{o}C is slightly different (192.8 J/g and 181.3 J/g respectively). This implies that the destruction of the raw material at 25^{o}C is slower, resulting in a slow polymerization process in which the destruction rate is suited to the polymerization rate [58]. As a result of this, a better geopolymeric material with good compressive strength is obtained.

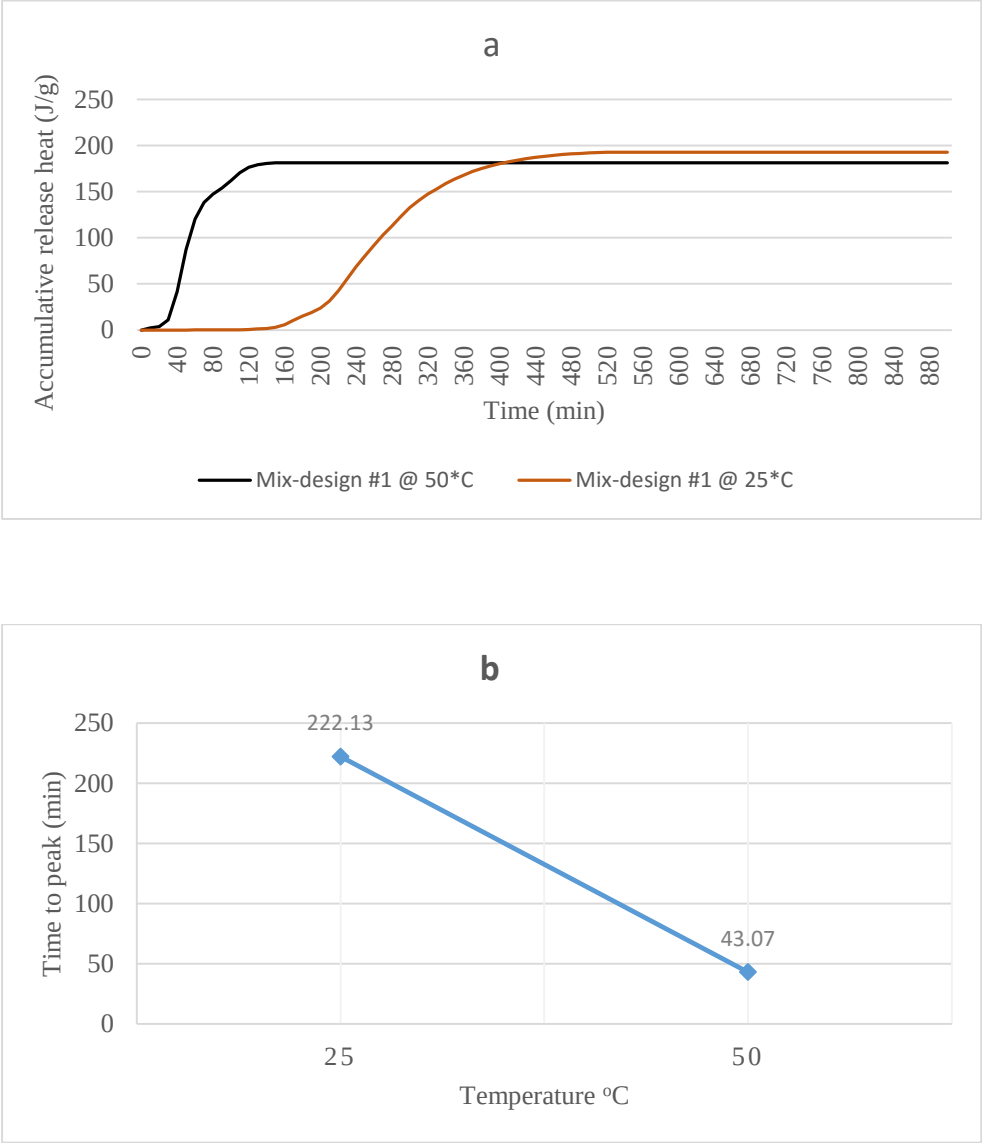

Fig 4.8: Relationship between temperature and: a) accumulative heat release rate and b) time to peak (gelation time).

Conversely, at 50°C the heat evolution is slightly shorter, which indicates that dissolution and the formation of oligomers and alumina/silica-hydroxy species is inefficient. This can be seen in the shorter gelation time in comparison to the system at 25°C, meaning that the time needed for the destruction of the raw material and the formation of the oligomers and alumina/silica-hydroxy species is not sufficient [87]. This shows that if the temperature rises above 50°C, the total heat evolution will continue to decrease, which implies the formation of large amounts of Si^{4+} and Al^{3+}

species at the surface of the raw material at the instant the aplite-slag particles are mixed with the activator. The material will immediately polymerize into gel, preventing further destruction of the raw material by covering on the particle surfaces [58].

4.6 Statistical variation

The results from each of the mix-designs relies solely on single experiments. The measured value is likely to deviate from the unknown, true value of the physical quantity (no measurement of a physical quantity can be entirely accurate). In addition to this, systematic errors may have been introduced during the experiments (for instance, from the operation/ calibration of the various instruments used, incorrect measuring technique etc.). Thus, the numerical values extracted cannot be treated statistically, and the reproducibility/ repeatability of these results has not been verified. Taking the above mentioned factors into account, the numerical values were rounded to four significant digits in order to make the numerical result more realistic.

In view of this, the experiment (for every mix-design) should ideally be repeated several times, to elucidate the statistical variation (random errors) of the results.

5

CONCLUSIONS AND RECOMMENDATIONS FOR FURTHER WORK

5.1 Conclusion

This chapter presents the main conclusion drawn from analyzing the thermal properties of geopolymer materials using isothermal and non-isothermal calorimetry technology.

The thermal characterization of the aplite-slag based geopolymer carried out in this thesis work is just a part of a larger project of the Petroleum Department at the University of Stavanger. The ongoing project considers several characterizations of this material, to access its utilization and full implementation in the oil and gas industry. Successful utilization and implementation of this material in actual industrial application will be beneficial in solving various issues related to industrial waste management and environmental pollution.

Based on the results from the thermal analyses, the following conclusions have been drawn from this project:

- The calorimetry curves of the geopolymerization process for an alkali-activated aplite-slag system showed either two or three distinguished exothermic peaks. The first peak indicates the dissolution of the aplite-slag particles, followed by a broad exothermic peak corresponding to the multi-step polymerization process of the dissolved Al and Si species in the aqueous phase. The third exothermic peak corresponds to gel reorganization/ transformation of the freshly formed geopolymeric products into fully cross-linked framework products.

- An increase in the (K_2SiO_3 + SiO_2) content decreases the accumulative heat release. This would greatly affect the mechanical properties of the material in a negative way. The most important conclusion of this research is that soluble silicon content in the geopolymerization process has a more pronounced effect on the extent of geopolymerization than does temperature. Hence, an appropriate elevation of (K_2SiO_3 + SiO_2) could improve the extent of the geopolymerization of raw materials.

- Raising the reaction temperature from 25^oC to 50^oC accelerated the reaction, but showed a slight effect on the polymerization extent (heat evolution). This suggests that an optimum reaction temperature could increase the polymerization extent and the extent of the reaction of the raw material.

- The addition of sucrose as an admixture in an aplite-slag based geopolymer has shown encouraging results, particularly in the improved accumulative heat release as compared to the non-sucrose mixture. In non-isothermal measurement, a 1.2% addition of sucrose to the mixture was found to be the optimum dosage, causing a 13.3% increase in the accumulative heat release compared to the non-sucrose mixture. Not only did the addition of 1.2% sucrose improve the accumulative heat release, but it also retarded the reaction rate of geopolymerization by prolonging the gelation period by up to 20.39 minutes as compared to the non-sucrose mixture.

It can then be concluded that the thermal analysis carried out on the aplite-slag based geopolymer has shown that mix-design #2 with 1.2% sucrose in the solid phase and a 0.431(K_2SiO_3 + SiO_2)/KOH ratio, is the optimum mix-design with optimum accumulative heat release, indicating better mechanical properties than the other mix-designs carried out in this experiment.

5.2 Recommendation for further work

There are several challenges in commercializing geopolymer technology. It has been observed that geopolymer performance depends solely on the properties of the source materials. Different geopolymer source materials have their own unique physical properties and chemical compositions, and therefore require different alkaline activator dosages and processing methods to attain similar mechanical performance. In addition, the same source material but from a different location will have different characteristic properties. Differences in the raw materials' properties will certainly hinder geopolymer knowledge from being transferred to industry practitioners.

In view of these challenges, further research is need to facilitate the implementation of the aplite-slag based geopolymer technology used in this thesis, in industrial application. The following is proposed:

- This thesis' experiment was carried out in an ideal laboratory environment, ignoring several factors such as elevated pressure, etc. Therefore, further research should be carried out under borehole rugged conditions (elevated pressure, confined space, etc.), to access the effect of those factors on the geopolymer's thermal properties.

- Thermal analysis on the long-term integrity of the geopolymer's final structure, by studying the material's thermal behavior and melting temperature.

- The effect of heat evolution on the steal tubulars casing integrity and on the borehole's temperature and pressure.

- The effect of contaminants such as drilling mud and borehole formation on the geopolymerization process and on the mechanical properties of the geopolymer's final structure.

- Spectroscopy techniques should be used to confirm the crystallization peaks' hypothesis given in Section 4.1 and to determine how the development of the crystal phase can be improved.

Appendix A

The geopolymer structure

A.1 Poly(sialates)

Sialate is an abbreviation for silicon-oxo-aluminate [11]. The framework of aluminosilicate geopolymeric gels is made up of a sialate network which consists of SiO_4 and AlO_4^-, tetrahedrally coordinated and linked by sharing all the oxygens. The negative charge on the AlO_4^- group is charged balance in a IV-fold coordination by the alkali cation that is present in the framework cavity [11]. This poly(sialates) ranges from an amorphous to a semi-crystalline three-dimensional aluminosilicate structure, termed "geopolymer," and is categorized based on the Si/Al ratio as shown in Figure A.1 [70].

The Si/Al ratio greatly affects the dissolution, hydrolysis, and condensation reaction of geopolymers. The condensation reaction in low Si/Al systems normally occurs between silica and alumina species, resulting in mainly poly(sialate) geopolymeric structures. On the other hand, in high Si/Al systems, the condensation reaction would occur predominantly within the silicate species itself, resulting in oligomeric silicate which then condenses with $Al(OH_4)^{4-}$, forming geopolymeric structures of poly(sialate-siloxo) and poly(sialate-disiloxo) [57, 104].

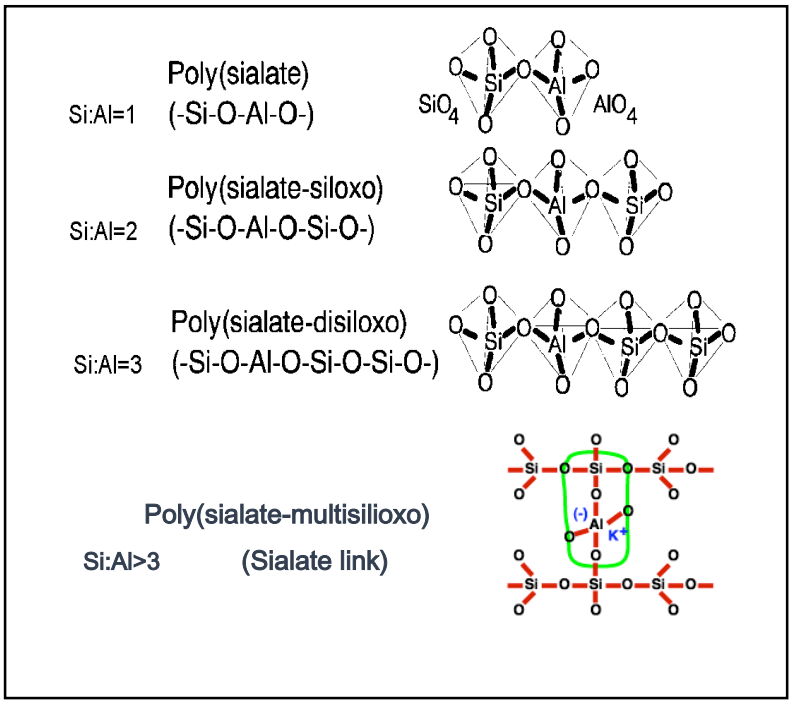

Figure A.1: The chemical structures of poly(sialates) [27].

A.1.1 Sialate, Poly(sialate) Si:Al = 1

(-Si-O-Al-O-) is a ring and chain of polymers resulting from the polycondensation of monomers, ortho-sialate $(OH)_3$-Si-O-Al-$(OH)_3$ [11].

A.1.2 Sialate-siloxo, Poly(sialate-siloxo) Si:Al = 2

(-Si-O-Al-O-Si-O-) is considered a polycondensation of orthosialate with ortho-silicic acid $Si(OH)_4$ [11].

A.1.3 Sialate-disiloxo, Poly(sialate-disiloxo) Si:Al = 3

(-Si-O-Al-O-Si-O-Si-O) is considered a polycondensation of orthosialate with two ortho-silicic acids $Si(OH)_4$ [11].

A.1.4 Silate link, Poly(sialate-multisilioxo) Si:Al >3

This stands for the bridge Si-O-Al between two poly(sialate) or poly(siloxonate) chains [11].

Table A-1: Applications of a geoplolymer material as related to its atomic Si/Al ratio [52].

Si:Al Ratio	Applications
1	• Bricks • Ceramics • Fire Protection
2	• Low CO_2 Cements and Concretes • Radioactive and Toxic Waste Encapsulation
3	• Fire Protection Fiberglass Composites • Foundry Equipment • Heat Resistant Composites, 200°C to 1000°C • Tooling for Aeronautics Titanium Process
>3	• Sealants for Industry, 200°C to 600°C • Tooling for Aeronautics SPF Aluminum
20-35	• Fire Resistant and Heat Resistant Fiber Composites

Appendix B

DSC dynamic segment curve and calibration curve

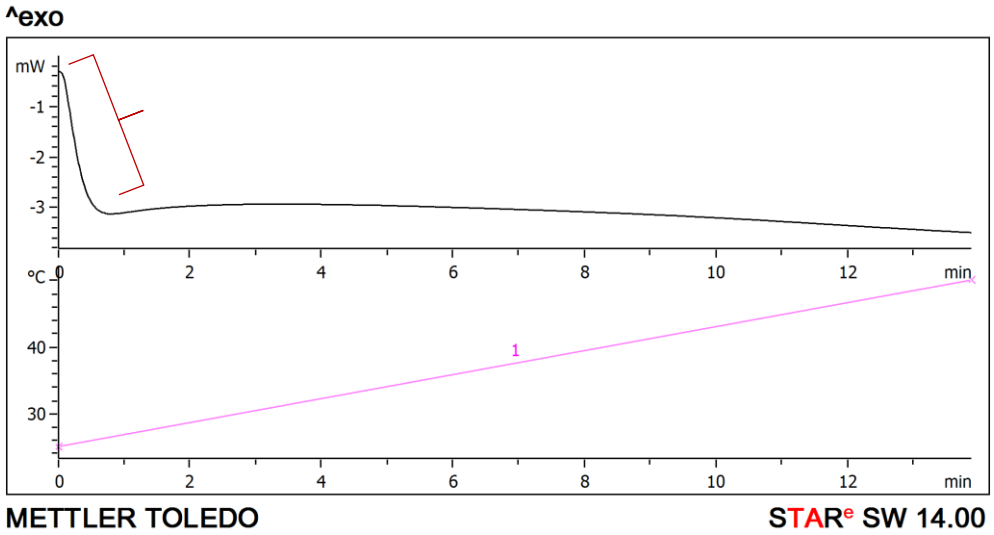

Fig B.1: DSC dynamic segment curve during the temperature ramp-up. The first few seconds show an endothermic start-up hook, indicating that the reference pan is too light to offset the sample. Hence, the first few seconds are not taken into account.

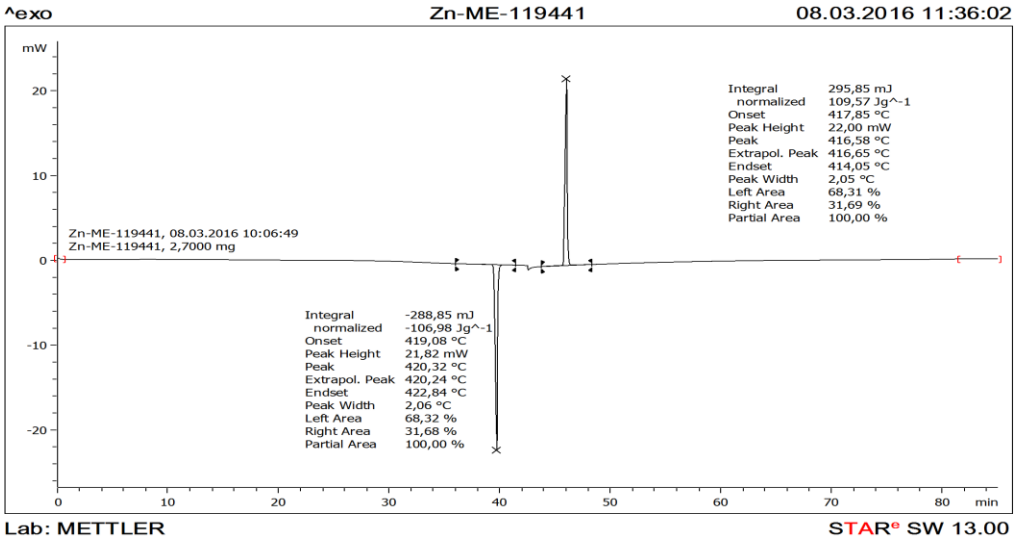

Fig B.2: Calibration curve of the DSC using zinc as the standard specimen. The measured curves correspond to the correct enthalpy of fussion/ melting point and enthalpy of crystallization/ crystallization point.

Appendix C

Advantages and disadvantages of DSC technique

It has been shown in this analysis that DSC is a useful technique for studying the geopolymerization process. However, there are also limitations associated with this technique.

The advantages and disadvantages are given below:

Advantages

- Wide range of temperature program
- Small amount of material is required
- High sensitivity
- Programmed heating/ cooling rates
- Clearness of result
- Any form of material can be analyzed

Disadvantages

- Highly sensitive to any changes
- The result depends mostly on the operator and the form of operation
- The rate of experiment cannot really be controlled
- Dependent on a lot of parameters

Appendix D

Accumulative heat release data of the mix-designs

Table D-1: Accumulative heat release.

Time (minute)	Sample 1 (J/g)	Sample 2 (J/g)	Sample 3 (J/g)	Sample 4 (J/g)	Sample 5 (J/g)	Sample 6 (J/g)	Sample 7 (J/g)	Sample 1 @25ºC (J/g)
0	0	0	0	0	0	0	0	0
10	2.25	2.45	1.78	1.28	2.02	1.57	3.13	0
20	3.69	4.26	2.53	1.56	2.65	4.4	4.18	0.01
30	10.87	12.56	6.81	3.87	3.33	16.04	6.84	0.01
40	41.57	25.41	18.11	8.13	4.58	43.37	11.69	0.02
50	87.14	46.06	29.9	16.71	6.66	83.65	18.24	0.03
60	120.21	78.69	48.45	26.92	9.18	121.6	25.87	0.04
70	138.36	122.74	74.41	38.75	11.91	142.14	33.68	0.05
80	147.35	149.46	111.74	52.63	15.02	150.75	40.41	0.06
90	153.91	164.73	142.23	69.74	17.86	154.99	46.58	0.07
100	161.92	173.58	157.03	90.81	20.6	157	51.21	0.09
110	170.66	180.04	165.09	112.71	23.2	157.76	52.95	0.33
120	176.46	186.58	171.82	127.54	25.15	158.08	53.04	0.64
130	179.22	192.35	178.01	139.49	26.87	158.23	53.04	1.08
140	180.71	198.28	182.14	148.35	27.64	158.23	53.04	1.77
150	181.14	201.58	185.08	152.78	27.81	158.23	53.04	3.09
160	181.19	203.78	187.14	154.74	27.82	158.23	53.04	5.77
170	181.28	204.81	188.77	155.73	27.82	158.23	53.04	10.5
180	181.28	205.33	189.73	155.99	27.82	158.23	53.04	14.99
190	181.28	205.46	190.19	156	27.82	158.23	53.04	18.83
200	181.28	205.46	190.43	156	27.82	158.23	53.04	23.72
210	181.28	205.46	190.52	156	27.82	158.23	53.04	31.52
220	181.28	205.46	190.53	156	27.82	158.23	53.04	42.44
230	181.28	205.46	190.53	156	27.82	158.23	53.04	55.84
240	181.28	205.46	190.53	156	27.82	158.23	53.04	68.7
250	181.28	205.46	190.53	156	27.82	158.23	53.04	80.34
260	181.28	205.46	190.53	156	27.82	158.23	53.04	91.78
270	181.28	205.46	190.53	156	27.82	158.23	53.04	102.84

280	181.28	205.46	190.53	156	27.82	158.23	53.04	112.49
290	181.28	205.46	190.53	156	27.82	158.23	53.04	122.87
300	181.28	205.46	190.53	156	27.82	158.23	53.04	132.72
310	181.28	205.46	190.53	156	27.82	158.23	53.04	140.37
320	181.28	205.46	190.53	156	27.82	158.23	53.04	147.22
330	181.28	205.46	190.53	156	27.82	158.23	53.04	152.86
340	181.28	205.46	190.53	156	27.82	158.23	53.04	158.76
350	181.28	205.46	190.53	156	27.82	158.23	53.04	163.53
360	181.28	205.46	190.53	156	27.82	158.23	53.04	167.76
370	181.28	205.46	190.53	156	27.82	158.23	53.04	171.74
380	181.28	205.46	190.53	156	27.82	158.23	53.04	174.94
390	181.28	205.46	190.53	156	27.82	158.23	53.04	177.94
400	181.28	205.46	190.53	156	27.82	158.23	53.04	180.34
410	181.28	205.46	190.53	156	27.82	158.23	53.04	182.45
420	181.28	205.46	190.53	156	27.82	158.23	53.04	184.14
430	181.28	205.46	190.53	156	27.82	158.23	53.04	185.93
440	181.28	205.46	190.53	156	27.82	158.23	53.04	187.23
450	181.28	205.46	190.53	156	27.82	158.23	53.04	188.33
460	181.28	205.46	190.53	156	27.82	158.23	53.04	189.34
470	181.28	205.46	190.53	156	27.82	158.23	53.04	190.21
480	181.28	205.46	190.53	156	27.82	158.23	53.04	190.9
490	181.28	205.46	190.53	156	27.82	158.23	53.04	191.48
500	181.28	205.46	190.53	156	27.82	158.23	53.04	191.9
510	181.28	205.46	190.53	156	27.82	158.23	53.04	192.31
520	181.28	205.46	190.53	156	27.82	158.23	53.04	192.55
530	181.28	205.46	190.53	156	27.82	158.23	53.04	192.71
540	181.28	205.46	190.53	156	27.82	158.23	53.04	192.79
550	181.28	205.46	190.53	156	27.82	158.23	53.04	192.8
560	181.28	205.46	190.53	156	27.82	158.23	53.04	192.8
570	181.28	205.46	190.53	156	27.82	158.23	53.04	192.8
580	181.28	205.46	190.53	156	27.82	158.23	53.04	192.8
590	181.28	205.46	190.53	156	27.82	158.23	53.04	192.8
600	181.28	205.46	190.53	156	27.82	158.23	53.04	192.8
610	181.28	205.46	190.53	156	27.82	158.23	53.04	192.8
620	181.28	205.46	190.53	156	27.82	158.23	53.04	192.8
630	181.28	205.46	190.53	156	27.82	158.23	53.04	192.8
640	181.28	205.46	190.53	156	27.82	158.23	53.04	192.8
650	181.28	205.46	190.53	156	27.82	158.23	53.04	192.8
660	181.28	205.46	190.53	156	27.82	158.23	53.04	192.8
670	181.28	205.46	190.53	156	27.82	158.23	53.04	192.8

680	181.28	205.46	190.53	156	27.82	158.23	53.04	192.8
690	181.28	205.46	190.53	156	27.82	158.23	53.04	192.8
700	181.28	205.46	190.53	156	27.82	158.23	53.04	192.8
710	181.28	205.46	190.53	156	27.82	158.23	53.04	192.8
720	181.28	205.46	190.53	156	27.82	158.23	53.04	192.8
730	181.28	205.46	190.53	156	27.82	158.23	53.04	192.8
740	181.28	205.46	190.53	156	27.82	158.23	53.04	192.8
750	181.28	205.46	190.53	156	27.82	158.23	53.04	192.8
760	181.28	205.46	190.53	156	27.82	158.23	53.04	192.8
770	181.28	205.46	190.53	156	27.82	158.23	53.04	192.8
780	181.28	205.46	190.53	156	27.82	158.23	53.04	192.8
790	181.28	205.46	190.53	156	27.82	158.23	53.04	192.8
800	181.28	205.46	190.53	156	27.82	158.23	53.04	192.8
810	181.28	205.46	190.53	156	27.82	158.23	53.04	192.8
820	181.28	205.46	190.53	156	27.82	158.23	53.04	192.8
830	181.28	205.46	190.53	156	27.82	158.23	53.04	192.8
840	181.28	205.46	190.53	156	27.82	158.23	53.04	192.8
850	181.28	205.46	190.53	156	27.82	158.23	53.04	192.8
860	181.28	205.46	190.53	156	27.82	158.23	53.04	192.8
870	181.28	205.46	190.53	156	27.82	158.23	53.04	192.8
880	181.28	205.46	190.53	156	27.82	158.23	53.04	192.8
890	181.28	205.46	190.53	156	27.82	158.23	53.04	192.8
900	181.28	205.46	190.53	156	27.82	158.23	53.04	192.8

Bibliography

[1] W. I. O. Środowiska. (2011). *Inspekcja Ochrony, Srodowiska*. Available: http://www.gios.gov.pl/stansrodowiska/gios/get_pdf/en/front/odpady

[2] W. K. Part, M. Ramli, and C. B. Cheah, "An overview on the influence of various factors on the properties of geopolymer concrete derived from industrial by-products," *Construction and Building Materials Construction and Building Materials*, vol. 77, pp. 370-395, 2015.

[3] *Guidelines on qualification of materials for the suspension and abandonment of wells*. London: Oil and Gas UK, 2012.

[4] H. Bolio and M. J. Conference: 13. international congress on the chemistry of cement, "Sustainable cement production-present and future," *Cement and Concrete Research*, vol. 41, pp. 642-650, 2011.

[5] S. Ahmari, X. Ren, V. Toufigh, and L. Zhang, "Production of geopolymeric binder from blended waste concrete powder and fly ash," *JCBM Construction and Building Materials*, vol. 35, pp. 718-729, 2012.

[6] P. Chindaprasirt, T. Chareerat, and V. Sirivivatnanon, "Workability and strength of coarse high calcium fly ash geopolymer," *CECO Cement and Concrete Composites*, vol. 29, pp. 224-229, 2007.

[7] J. Davidovits, s. Conference: 5. global warming, c. policy international, and S. F. C. A. A. expo, "Global warming impact on the cement and aggregates industries," *World Resource Review*, vol. 6:2, pp. 263-278, 1994.

[8] J. S. Damtoft, J. Lukasik, D. Herfort, D. Sorrentino, and E. M. Gartner, "Sustainable development and climate change initiatives," *CEMCON Cement and Concrete Research*, vol. 38, pp. 115-127, 2008.

[9] A. Allahverdi and E. Najafi Kani, "Construction wastes as raw materials for geopolymer binders," *Int. J. Civ. Eng. International Journal of Civil Engineering*, vol. 7, pp. 154-160, 2009.

[10] H. Zhu and X. Yao, "Effect of retarder on reaction process of metakaolin-slag-based geopolymer," *J. Theor. Appl. Inf. Technol. Journal of Theoretical and Applied Information Technology*, vol. 48, pp. 1384-1390, 2013.

[11] J. Davidovits, *Geopolymer chemistry and applications*. Saint-Quentin: Institut Géopolymère, 2008.

[12] M. Lizcano, H. S. Kim, S. Basu, and M. Radovic, "Mechanical properties of sodium and potassium activated metakaolin-based geopolymers," *J Mater Sci Journal of Materials Science : Full Set - Includes `Journal of Materials Science Letters'*, vol. 47, pp. 2607-2616, 2012.

[13] Q. Wang, K. Ran, Z. Ding, L. Qiu, International Conference on Mechanical Engineering, and M. Manufacturing Engineering, "Research on mechanical properties of geopolymer concrete under early stage curing system," *Appl. Mech. Mater. Applied Mechanics and Materials*, vol. 164, pp. 492-496, 2012.

[14] S. Aydin and B. Baradan, "Mechanical and microstructural properties of heat cured alkali-activated slag mortars," *JMAD Materials and Design*, vol. 35, pp. 374-383, 2012.

[15] A. Islam, U. J. Alengaram, M. Z. Jumaat, and I. I. Bashar, "The development of compressive strength of ground granulated blast furnace slag-palm oil fuel ash-fly ash based geopolymer mortar," *JMAD Materials and Design*, vol. 56, pp. 833-841, 2014.

[16] A. Nazari, A. Bagheri, and S. Riahi, "Properties of geopolymer with seeded fly ash and rice husk bark ash," *MSA Materials Science & Engineering A*, vol. 528, pp. 7395-7401, 2011.

[17] G. Gorhan and G. Kurklu, "The influence of the NaOH solution on the properties of the fly ash-based geopolymer mortar cured at different temperatures," *Compos Part B: Eng Composites Part B: Engineering*, vol. 58, pp. 371-377, 2014.

[18] H. M. Giasuddin, J. G. Sanjayan, and P. G. Ranjith, "Strength of geopolymer cured in saline water in ambient conditions," *JFUE Fuel*, vol. 107, pp. 34-39, 2013.

[19] J. He, G. Zhang, Y. Jie, J. Zhang, and Y. Yu, "Synthesis and characterization of red mud and rice husk ash-based geopolymer composites," *Cem Concr Compos Cement and Concrete Composites*, vol. 37, pp. 108-118, 2013.

[20] Y. Chen, Y. Zhang, T. Chen, Y. Zhao, and S. Bao, "Preparation of eco-friendly construction bricks from hematite tailings," *JCBM Construction and Building Materials*, vol. 25, pp. 2107-2111, 2011.

[21] S. Ahmari and L. Zhang, "Production of eco-friendly bricks from copper mine tailings through geopolymerization," *JCBM Construction and Building Materials*, vol. 29, pp. 323-331, 2012.

[22] A. Kusbiantoro, M. S. Ibrahim, K. Muthusamy, and A. Alias, "Development of Sucrose and Citric Acid as the Natural based Admixture for Fly Ash based Geopolymer," *PROENV Procedia Environmental Sciences*, vol. 17, pp. 596-602, 2013.

[23] M. Khalifeh, A. Saasen, T. Vrålstad, H. B. Larsen, and H. Hodne, "Experimental study on the synthesis and characterization of aplite rock-based geopolymers," *Journal of Sustainable Cement-Based Materials*, vol. 5, pp. 233-246, 2016.

[24] H. Rahier, B. Van Mele, M. Biesemans, J. Wastiels, and X. Wu, "Low-temperature synthesized aluminosilicate glasses : Part I Low-temperature reaction stoichiometry and structure of a model compound," *JOURNAL OF MATERIALS SCIENCE Journal of Materials Science*, vol. 31, pp. 71-79, 1996.

[25] M. Wagner and G. Widmann, *Thermal analysis in practice*. Schwerzenbach: Mettler-Toledo, 2009.

[26] J. L. Provis and J. S. J. Van Deventer, "Geopolymers structure, processing, properties and industrial applications," ed Oxford; Boca Raton, FL: Woodhead ; CRC Press, 2009, pp. 1-100.

[27] J. Davidovits, "30 Years of Successes and Failures in Geopolymer Applications.," presented at the Geopolymer 2002 Conference, October 28-29, 2002, Melbourne, Australia, 2002.

[28] J. Bell, M. Gordon, and W. Kriven, "Use of Geopolymeric Cements as a Refractory Adhesive for Metal and Ceramic Joins," *CERAMIC ENGINEERING AND SCIENCE PROCEEDINGS*, vol. 26, pp. 407-414, 2005.

[29] P. V. Krivenko and G. Y. Kovalchuk, "Directed synthesis of alkaline aluminosilicate minerals in a geocement matrix," *J Mater Sci Journal of Materials Science : Full Set - Includes `Journal of Materials Science Letters'*, vol. 42, pp. 2944-2952, 2007.

[30] J. Wastiels, X. Wu, S. Faignet, and G. Patfoort, "Mineral Polymer Based on Fly Ash," *JOURNAL OF RESOURCE MANAGEMENT AND TECHNOLOGY*, vol. 22, p. 135, 1994.

[31] M. European Conference on Soft, C. Université de technologie de, and I. Geopolymer, *Geopolymer '88 : first European Conference on Soft Mineralurgy[sic], Compiegne, France, June 1988*, 1988.

[32] J. Davidovits, "High-alkali cements for 21st century concretes," *Special Publication*, vol. 144, pp. 383-398, 1994.

[33] D. Hardjito, S. E. Wallah, D. M. J. Sumajouw, and B. Vijaya Rangan, "On the Development of Fly Ash-Based Geopolymer Concrete," *ACI materials journal.*, vol. 101, p. 467, 2004.

[34] D. C. Comrie, J. H. Paterson, and D. C. Ritcey, "Geopolymer technologies in toxic waste management," in *1st European Conference on Soft Mineralogy*, Compiegne, France., 1988, pp. 107-124, 1988.

[35] D. L. Y. Kong and J. G. Sanjayan, "Damage behavior of geopolymer composites exposed to elevated temperatures," *CECO Cement and Concrete Composites*, vol. 30, pp. 986-991, 2008.

[36] J. Temuujin, A. van Riessen, and R. Williams, "Influence of calcium compounds on the mechanical properties of fly ash geopolymer pastes," *JOURNAL OF HAZARDOUS MATERIALS*, vol. 167, pp. 82-88, 2009.

[37] H. Xu and J. S. J. Van Deventer, "Geopolymerisation of multiple minerals," *MINE Minerals Engineering*, vol. 15, pp. 1131-1139, 2002.

[38] H. Xu and J. S. J. Van Deventer, "The geopolymerisation of alumino-silicate minerals," *MINPRO International Journal of Mineral Processing*, vol. 59, pp. 247-266, 2000.

[39] J. C. Swanepoel and C. A. Strydom, "Utilisation of fly ash in a geopolymeric material," *Applied Geochemistry*, vol. 17, pp. 1143-1148, 2002.

[40] V. F. Barbosa, K. J. MacKenzie, and C. Thaumaturgo, "Synthesis and characterisation of materials based on inorganic polymers of alumina and silica: sodium polysialate polymers," *INTERNATIONAL JOURNAL OF INORGANIC MATERIALS*, vol. 2, pp. 309-317, 2000.

[41] D. Khale and R. Chaudhary, "Mechanism of geopolymerization and factors influencing its development: a review," *J Mater Sci Journal of Materials Science : Full Set - Includes `Journal of Materials Science Letters'*, vol. 42, pp. 729-746, 2007.

[42] E. G. Nawy, *Concrete construction engineering handbook*. Boca Raton: CRC Press, 2008.

[43] A. M. M. A. Bakri, H. Kamarudin, M. N. Norazian, C. M. Ruzaidi, Y. Zarina, and A. R. Rafiza, "Microstructure Studies on the Effect of the Alkaline Activators Ratio in Preparation of Fly Ash-Based Geopolymer," presented at the International Conference on Chemistry and Chemical Process, Singapore, 2011.

[44] J. Xie, J. Yin, J. Chen, and J. Xu, "Study on the Geopolymer Based on Fly Ash and Slag," presented at the International Conference on, Energy, Environment, Technology, 2009.

[45] S. P. Thakkar, D. J. Bhorwani, and R. Ambaliya, "Geopolymer Concrete Using Different Source Materials," *International Journal of Emerging Technology and Advanced Engineering*, vol. 4, pp. 10-16, 2014.

[46] D. Dutta and S. Ghosh, "The effect of Na2O concentration in activator for fly ash based Geopolymer blended with slag," *International Journal of Applied Sciences and Engineering Research*, vol. 3, 2014.

[47] U. Rattanasak, K. Pankhet, and P. Chindaprasirt, "Effect of chemical admixtures on properties of high-calcium fly ash geopolymer," *Int J Miner Metall Mater International Journal of Minerals, Metallurgy, and Materials*, vol. 18, pp. 364-369, 2011.

[48] T. Bakharev, J. G. Sanjayan, and Y. B. Cheng, "Alkali activation of Australian slag cements," *Cement and Concrete Research. Jan.1999*, vol. 29, pp. 113-120, 1999.

[49] F. Pacheco-Torgal, J. Castro-Gomes, and S. Jalali, "Alkali-activated binders: A review. Part 2. About materials and binders manufacture," *Constr Build Mater Construction and Building Materials*, vol. 22, pp. 1315-1322, 2008.

[50] Wikipedia. (2012). *Apilte rock.* Available: https://en.wikipedia.org/wiki/Aplite

[51] P. Duxson, A. Fernández-Jiménez, J. L. Provis, G. C. Lukey, A. Palomo, and J. S. J. van Deventer, "Geopolymer technology: the current state of the art," *J Mater Sci Journal of Materials Science : Full Set - Includes `Journal of Materials Science Letters'*, vol. 42, pp. 2917-2933, 2007.

[52] J. C. Petermann, A. Saeed, and M. I. Hammond, "Alkali-Activated Geopolymers: A Literature Review," A. F. R. L. M. A. M. DIRECTORATE, Ed., ed: APPLIED RESEARCH ASSOCIATES INC PANAMA CITY FL, 2010.

[53] P. C. Hewlett and A. Cement Admixtures, "Cement admixtures : uses and applications," ed Harlow: Longman Scientific & Technical, 1988, pp. 1-5.

[54] Bigpicture. (2015). *Carbon's central role.* Available: http://bigpictureeducation.com/carbons-central-role

[55] V. D. Glukhovsky, *Soil silicates (Gruntosilikaty)*, . Kiev: USSR: Budivelnik publisher, 1959.

[56] H. Rahier, J. Wastiels, M. Biesemans, R. Willlem, G. Van Assche, and B. Van Mele, "Reaction mechanism, kinetics and high temperature transformations of geopolymers," *J Mater Sci Journal of Materials Science : Full Set - Includes `Journal of Materials Science Letters'*, vol. 42, pp. 2982-2996, 2007.

[57] P. D. Silva, K. Sagoe-Crenstil, and V. Sirivivatnanon, "Kinetics of geopolymerization: Role of Al2O3 and SiO2," *CEMCON Cement and Concrete Research,* vol. 37, pp. 512-518, 2007.

[58] X. Yao, Z. Zhang, H. Zhu, and Y. Chen, "Geopolymerization process of alkalimetakaolinite characterized by isothermal calorimetry," *Thermochimica Acta Thermochimica Acta,* vol. 493, pp. 49-54, 2009.

[59] Z. Zhang, H. Wang, J. L. Provis, F. Bullen, A. Reid, and Y. Zhu, "Quantitative kinetic and structural analysis of geopolymers. Part 1. The activation of metakaolin with sodium hydroxide," *TCA Thermochimica Acta,* vol. 539, pp. 23-33, 2012.

[60] A. Fernandez-Jimenez, A. Palomo, and M. Criado, "Microstructure development of alkali-activated fly ash cement: a descriptive model," *Cement and concrete research.,* vol. 35, p. 1204, 2005.

[61] A. Fernández-Jiménez, A. Palomo, I. Sobrados, and J. Sanz, "The role played by the active alumina content in the alkaline activation of fly ashes," *Microporous and Mesoporous Material,* vol. 91, pp. 111-119, 2006.

[62] J. L. Provis, G. C. Lukey, and J. S. J. van Deventer, "Do Geopolymers Actually Contain Nanocrystalline Zeolites? A Reexamination of Existing Results," *CHEMISTRY OF MATERIALS,* vol. 17, pp. 3075-3085, 2005.

[63] J. S. J. van Deventer, J. L. Provis, P. Duxson, and G. C. Lukey, "Reaction mechanisms in the geopolymeric conversion of inorganic waste to useful products," *HAZMAT Journal of Hazardous Materials,* vol. 139, pp. 506-513, 2007.

[64] J. L. Provis, E. American Institute of Chemical, and M. Annual, "Modeling the formation of geopolymers," ed. New York, N.Y.: distributed by American Institute of Chemical Engineers, 2006.

[65] P. Duxson, "Structure and Thermal Conductivity of Metakaolin Geopolymers," Ph.D. Thesis, Department of Chemical & Biomolecular Engineering, University of Melbourne, Australia, 2006.

[66] E. H. Oelkers, J. Schott, and J.-L. Devidal, "The effect of aluminum, pH, and chemical affinity on the rates of aluminosilicate dissolution reactions," *GCA Geochimica et Cosmochimica Acta,* vol. 58, pp. 2011-2024, 1994.

[67] E. H. Oelkers and S. R. Gislason, "The mechanism, rates and consequences of basaltic glass dissolution: I. An experimental study of the dissolution rates of basaltic glass as a function of aqueous Al, Si and oxalic acid concentration at 25°C and pH = 3 and 11," *GCA Geochimica et Cosmochimica Acta,* vol. 65, pp. 3671-3681, 2001.

[68] P. Duxson, J. L. Provis, G. C. Lukey, F. Separovic, and J. S. van Deventer, "29Si NMR study of structural ordering in aluminosilicate geopolymer gels," *Langmuir : the ACS journal of surfaces and colloids*, vol. 21, pp. 3028-36, 2005.

[69] P. Duxson, J. L. Provis, G. C. Lukey, S. W. Mallicoat, W. M. Kriven, and J. S. J. van Deventer, "Understanding the relationship between geopolymer composition, microstructure and mechanical properties," *Colloids and Surfaces A: Physicochemical and Engineering Aspects Colloids and Surfaces A: Physicochemical and Engineering Aspects*, vol. 269, pp. 47-58, 2005.

[70] J. Davidovits, "Properties of geopolymer cements," in *1st International Conference on Alkaline Cements and Concretes Conference, scientific research institute on binders and materials, Kiev state technical university*, Kiev, Ukraine, 1994, pp. 1-17.

[71] J. G. S. Van Jaarsveld, J. S. J. Van Deventer, and L. Lorenzen, "The potential use of geopolymeric materials to immobilise toxic metals: Part I. Theory and applications," *MINE Minerals Engineering*, vol. 10, pp. 659-669, 1997.

[72] B. V. Rangan, "Fly Ash-Based Geopolymer Concrete," in *the International Workshop on Geopolymer Cement and Concrete*, Mumbai, India, 2010, pp. 68-106.

[73] J. Davidovits, "Synthesis of New- High Temperature Geo-polymer for Reinforce plastic/composites," *SPE PACTEC '79, society of plastic Engineer, Brookfield center, USA,* pp. 151-154, 1979.

[74] J. Sestak, "Thermal science and analysis: Terms connotation, history, development, and the role of personalities," *J Therm Anal Calor Journal of Thermal Analysis and Calorimetry*, vol. 113, pp. 1049-1054, 2013.

[75] G. W. H. Höhne, W. F. Hemminger, and H. J. Flammersheim, *Differential Scanning Calorimetry*, Second revised and enlarge edition ed. Berlin, Heidelberg: Springer Berlin Heidelberg, 2003.

[76] "Differential Scanning Calorimetry; First and Second Order Transitions in Polymers," Department of Chemistry, colby college, 5750 Mayflower Hill, Waterville, Maine 04901, Available: http://www.colby.edu/chemistry/PChem/lab/DiffScanningCal.pdf, 2011.

[77] P. Gabbott, *Principles and applications of thermal analysis*. Oxford; Ames, Iowa: Blackwell Pub., 2008.

[78] H. Rahier, B. Wullaert, and B. Van Mele, "Influence of the Degree of Dehydroxylation of Kaolinite on the Properties of Aluminosilicate Glasses," *Journal of Thermal Analysis and Calorimetry Journal of Thermal Analysis and Calorimetry : An International Forum for Thermal Studies*, vol. 62, pp. 417-427, 2000.

[79] J. W. Phair, J. S. J. Van Deventer, and J. D. Smith, "Interaction of sodium silicate with zirconia and its consequences for polysialation," *COLSUA Colloids and Surfaces A: Physicochemical and Engineering Aspects*, vol. 182, pp. 143-159, 2001.

[80] M. L. Granizo, S. Alonso, M. T. Blanco-Varela, and A. Palomo, "Alkaline Activation of Metakaolin: Effect of Calcium Hydroxide in the Products of Reaction," *JACE Journal of the American Ceramic Society*, vol. 85, pp. 225-231, 2002.

[81] R. Cioffi, L. Maffucci, and L. Santoro, "Optimization of geopolymer synthesis by calcination and polycondensation of a kaolinitic residue," *Resources, Conservation and Recycling Resources, Conservation and Recycling*, vol. 40, pp. 27-38, 2003.

[82] S. Alonso and A. Palomo, "Alkaline activation of metakaolin and calcium hydroxide mixtures: influence of temperature, activator concentration and solids ratio," *Materials Letters Materials Letters*, vol. 47, pp. 55-62, 2001.

[83] H. Rahier, J. F. Denayer, and B. van Mele, "Low-temperature synthesized aluminosilicate glasses Part IV Modulated DSC study on the effect of particle size of metakaolinite on the production of inorganic polymer glasses," *Journal of Materials Science Journal of Materials Science*, vol. 38, pp. 3131-3136, 2003.

[84] J. L. Provis, "Modelling the formation of geopolymers," Ph. D, Dept. of Chemical and Biomolecular Engineering, University of Melbourne, Australia, 2006.

[85] M. L. Granizo, M. T. Blanco-Varela, and A. Palomo, "Influence of the starting kaolin on alkali-activated materials based on metakaolin. Study of the reaction parameters by isothermal conduction calorimetry," *Journal of Materials Science Journal of Materials Science*, vol. 35, pp. 6309-6315, 2000.

[86] J. G. S. van Jaarsveld, J. S. J. van Deventer, and G. C. Lukey, "The effect of composition and temperature on the properties of fly ash- and kaolinite-based geopolymers," *CEJ Chemical Engineering Journal*, vol. 89, pp. 63-73, 2002.

[87] M. S. Muñiz-Villarreal, A. Manzano-Ramírez, S. Sampieri-Bulbarela, J. R. Gasca-Tirado, J. L. Reyes-Araiza, J. C. Rubio-Ávalos, *et al.*, "The effect of temperature on the geopolymerization process of a metakaolin-based geopolymer," *MLBLUE Materials Letters*, vol. 65, pp. 995-998, 2011.

[88] Z. Zhang, H. Wang, F. Bullen, J. L. Provis, and A. Reid, "Quantitative kinetic and structural analysis of geopolymers. Part 2. Thermodynamics of sodium silicate activation of metakaolin," *Thermochim Acta Thermochimica Acta*, vol. 565, pp. 163-171, 2013.

[89] J. G. S. van Jaarsveld and J. S. J. van Deventer, "Effect of the Alkali Metal Activator on the Properties of Fly Ash-Based Geopolymers," *Ind. Eng. Chem. Res. Industrial & Engineering Chemistry Research*, vol. 38, pp. 3932-3941, 1999.

[90] K. Srinivasan and A. Sivakumar, "Geopolymer Binders: A Need for Future Concrete Construction," *ISRN.PS ISRN Polymer Science*, vol. 2013, 2013.

[91] P. Duxson, G. C. Lukey, F. Separovic, and J. S. J. van Deventer, "Effect of Alkali Cations on Aluminum Incorporation in Geopolymeric Gels," *INDUSTRIAL AND ENGINEERING CHEMISTRY RESEARCH*, vol. 44, pp. 832-839, 2005.

[92] H. E. Mc Gannon and C. United States Steel, *The making,shaping and treating of steel : 9th ed*. Pittsburgh,Pennsylvania: United States Steel, 1971.

[93] T. Bakharev, "Alkali activated slag concrete : chemistry, microstructure and durability," Ph.D, Department of Civil, Engineering, Monash, Universit, 2000.

[94] B. Talling and J. Brandstetr, "Present state and future of alkali-activated slag concretes," *Special Publication,* vol. 114, pp. 1519-1546, 1989.

[95] J. J. Chang, "A study on the setting characteristics of sodium silicate-activated slag pastes," *CEMCON Cement and Concrete Research,* vol. 33, pp. 1005-1011, 2003.

[96] U. Sharmaa, A. Khatrib, and A. Kanoungoc, "Use of Micro-silica as Additive to Concrete," *International Journal of Civil Engineering Research,* vol. 4, pp. 9-12, 2014.

[97] API.10B-2, *Recommended practice for testing well cements*. Washington, D.C.: API Publishing Services, 2005.

[98] D. Ravikumar and N. Neithalath, "Reaction kinetics in sodium silicate powder and liquid activated slag binders evaluated using isothermal calorimetry," *TCA Thermochimica Acta,* vol. 546, pp. 32-43, 2012.

[99] C. Shi and R. L. Day, "A calorimetric study of early hydration of alkali-slag cements," *CEMCON Cement and Concrete Research,* vol. 25, pp. 1333-1346, 1995.

[100] ASTM.D3418-15, *Standard test method for transition temperatures and enthalpies of fusion and crystallization of polymers by differential scanning calorimetry*. West Conshohocken, PA: ASTM International, 2012.

[101] ASTM.E968-02, *Standard Practice for Heat Flow Calibration of Differential Scanning Calorimeters*: ASTM international, 2014.

[102] L. C. Thomas, "Interpreting unexpected events and transitions in DSC results," *Technical publication TA-039, TA Instruments,* 2000.

[103] M. Schubnell, *Thermal analysis, information for users, usercom,* 40th ed. Schwerzenbach: Mettler-Toledo, 2014.

[104] M. R. North and T. W. Swaddle, "Kinetics of Silicate Exchange in Alkaline Aluminosilicate Solutions," *Inorg. Chem. Inorganic Chemistry,* vol. 39, pp. 2661-2665, 2000.